Results in Physics 19 (2020) 103684

Contents lists available at ScienceDirect

Results in Physics

journal homepage: www.elsevier.com/locate/rinp

On the interaction between (low & high) frequency of (ion-acoustic & Langmuir) waves in plasma via some recent computational schemes

Mostafa M.A. Khater [a,b,1], Raghda A.M. Attia [a,b,1], Emad E. Mahmoud [c,d,1], Abdel-Haleem Abdel-Aty [e,f,1,*], Kholod M. Abualnaja [g,1], A.-B.A. Mohamed [h,i,1], Hichem Eleuch [j,k,l,1]

[a] Department of Mathematics, Faculty of Science, Jiangsu University, 212013, Zhenjiang, China
[b] Department of Basic Science, Higher Technological Institute, 10th of Ramadan City 44629, Sharkia, Egypt
[c] Department of Mathematics and Statistics, College of Science, Taif University, P.O. Box 11099, Taif 21944, Saudi Arabia
[d] Department of Mathematics, Faculty of Science, Sohag University, Sohag 82524, Egypt
[e] Department of Physics, College of Sciences, University of Bisha, P.O. Box 344, Bisha 61922, Saudi Arabia
[f] Physics Department, Faculty of Science, Al-Azhar University, Assiut 71524, Egypt
[g] Department of Mathematics, Faculty of Applied Science, Umm Al-Qura University, P.O. Box 14949, Makkah, Saudi Arabia
[h] Department of Mathematics, College of Science and Humanities in Al-Aflaj, Prince Sattam Bin Abdulaziz University, Al-Aflaj, Saudi Arabia
[i] Department of Mathematics, Faculty of Science, Assiut University, Assiut, Egypt
[j] Department of Applied Physics and Astronomy, University of Sharjah, Sharjah, United Arab Emirates
[k] Department of Applied Sciences and Mathematics, College of Arts and Sciences, Abu Dhabi University, Abu Dhabi 59911, United Arab Emirates
[l] Institute for Quantum Science and Engineering, Texas A&M University, College Station, TX 77843, USA

ARTICLE INFO

MSC:
26A33
34A08
35B40

Keywords:
The dimensionless form of the Zakharov (ZE) equation
The high-frequency Langmuir waves
The low-frequency ion-acoustic waves
Computational schemes
Solitonary Solutions
Stability property

ABSTRACT

Applying several latest theoretical techniques, the empirical description of the interaction between the high-frequency Langmuir and the low-frequent ion-acoustic waves, derived mathematically by Zakharov's non-dimensional (ZE) equation. These interactions are described in electromagnetic waves, plasma physics, signal processing through optical fibers, coastal engineering, and fluid dynamics. Three modern computing methods are being used to construct several solutions: the extended exp(ϕ)-expansion process, the popular Kudryashov process, and the modified Khather method. Centered on the properties of the Hamilton system, the stability properties of the solutions are investigated. The physical proprieties are illustrated using 3D plots. The originality of the obtained solutions is explored. We demonstrate that we retrieve the old known solutions and we obtain new solutions that have never been found before.

1. Introduction

The dynamics of several natural phenomena at small scales is described by the partial differential equations (PDEs) [1]. For example, the electrical and mechanical proprieties of materials has been explored by solving PDEs [2–4]. PDEs are also governing the dynamics in solid-state physics, [5] plasma physics, [6,7] chemical kinematics, fibers [8, 9], control theory, [10,11], signal processing, electro-circuits [12], biogenetics [13,14], cell recognition [15], cell detection [16], non-linear optics [17,18], Quantum mechanics [19,20] and fluid movement [21, 22]. Due to the increasing need for closed-form solutions that allow the investigation of many phenomena in the above-mentioned areas, the PDE research field is becoming very active [23–26].

Furthermore not only analytical but also numerical solutions of PDEs become now essential tools for analyzing and simulating complex structures and phenomena in physics [27–34]. Consequently, various systematic techniques have been suggested as useful methods to investigate the closed-form solutions for many physical phenomena, such as the vector iteration method, the Adomian decomposition technique, the homotopic disruption method, the finite element protocol, the ex-function method, the Riccati expansion mechanism, the sech–tanh Method, and so on [35–41].

* Corresponding author at: Department of Physics, College of Sciences, University of Bisha, P.O. Box 344, Bisha 61922, Saudi Arabia.
E-mail address: amabdelaty@ub.edu.sa (A.-H. Abdel-Aty).
[1] All authors have equal contribution in this manuscript.

https://doi.org/10.1016/j.rinp.2020.103684
Received 2 October 2020; Received in revised form 27 November 2020; Accepted 28 November 2020
Available online 1 December 2020

Here we are using a mathematical model explains the relationship between the Langmuir high frequency and the acoustic waves [42, 43] of low frequency. This mechanism is defined mathematically by Zakharov's dimensionless type, derived from Zakharov [44,45]. This equation is given by [46]

$$\begin{cases} \imath\,\mathfrak{P}_t + \mathfrak{P}_{xx} + w_1\,\Psi\left(|\mathfrak{P}|^2\right)\mathfrak{P} = \mathfrak{P}\,\varphi, \\ \varphi_{tt} - \varphi_{xx} = \left(|\mathfrak{P}|^{2\gamma}\right)_{xx}, \end{cases} \tag{1}$$

where $\left[\mathfrak{P} = \mathfrak{P}(x,t),\ \varphi = \varphi(x,t)\right]$ respectively, represent the envelope of the high-frequency electric field and the plasma density. While w_1 is arbitrary constant.

For $\left[\Psi\left(|\mathfrak{P}|^2\right) = |\mathfrak{P}|^2,\ \gamma = 1\right]$, Eq. (1) becomes

$$\begin{cases} \imath\,\mathfrak{P}_t + \mathfrak{P}_{xx} + w_1\,|\mathfrak{P}|^2\,\mathfrak{P} = \mathfrak{P}\,\varphi, \\ \varphi_{tt} - \varphi_{xx} = \left(|\mathfrak{P}|^2\right)_{xx}, \end{cases} \tag{2}$$

Using the following transformation $\left[\mathfrak{P} = \Upsilon\,e^{\imath\,\vartheta},\ \Upsilon = \Upsilon(\mathfrak{F}),\ \mathfrak{F} =, x - r_1\,t,\ \vartheta = -r_2\,x + r_3\,t + r_4 \text{where } r_i,\ (i = 1,2,3,4) \text{ are arbitrary constants.}\right]$ on Eq. (2), leads to

$$\begin{cases} \left(\imath\,r_1\,\Upsilon' - r_3\,\Upsilon + \Upsilon'' - 2\,\imath\,r_2\,\Upsilon' - r_2^2\,\Upsilon + w_1\,\Upsilon^3 - \Upsilon\,\varphi\right)e^{\imath\,\vartheta} = 0, \\ \left(r_1^2 - 1\right)\varphi'' - \left(\Upsilon^2\right)'' = 0. \end{cases} \tag{3}$$

For $(r_1 + 2\,r_2 = 0)$ and twice integration of the second equation in Eq. (3) with zero constant of integration then substituting the result into first equation of the same system, yields

$$\Upsilon'' - q_1\,\Upsilon + q_2\,\Upsilon^3 = 0, \tag{4}$$

where $\left[q_1 = r_3 + r_2^2,\ q_2 = \left(w_1 - \frac{1}{r_1^2 - 1}\right)\right]$. Using the homogeneous balance principles on Eq. (4), yields $\left[n + 1 = m\right]$. So that, the explicit solutions of Eq. (4) takes many explicit expressions with respect to the values of n, m. For simplification, we take the following values of them $\left[n = 1\ \&\ m = 2\right]$.

The goal of our research paper is investigating the solitary solutions of the dimensionless form of the Zakharov equation via three recent analytical schemes to explain distinct types of computational solutions. These solutions are deeply helpful to explore more physical and dynamical behavior of the plasma hydrodynamics as well as their further applications in practical life.

The remaining parts of this paper are presented as: Three latest computational schemes are used in Section 2 to determine separate formulations of the dimensionless version of the Zakharov equation and are presented in various forms. In Section 3, we analyze the stability property of the obtained solutions. In Section 4, figures of the obtained solution are illustrated. In Section 5, the novelty of our paper is discussed. We end up by a conclusion in Section 6.

2. Explicit wave solutions of the dimensionless form of the Zakharov equation

In this section, we try to find some distinct stationary wave solutions of Eq. (1) via applying three recent analytical schemes.

2.1. The extended exp(ϕ)-expansion method

By Using the extended exp(ϕ)-expansion method, we obtain the general solutions of Eq. (4) as:

$$\Upsilon(\mathfrak{F}) = \frac{\sum_{i=0}^{m} a_i\,e^{-i\phi(\mathfrak{F})}}{\sum_{i=0}^{n} b_i\,e^{-i\phi(\mathfrak{F})}} = \frac{a_1\,e^{-\phi(\mathfrak{F})} + a_2\,e^{-2\phi(\mathfrak{F})} + a_0}{b_1\,e^{-\phi(\mathfrak{F})} + b_0}, \tag{5}$$

where $\left[a_0,\ a_1,\ a_2,\ b_0,\ b_1\right]$ are arbitrary constants. Also, $\phi(\mathfrak{F})$ is the solution function of the following ordinary differential equation

$$\phi'(\mathfrak{F}) = s_2\,e^{\phi(\mathfrak{F})} + \frac{s_3}{e^{\phi(\mathfrak{F})}} + s_1, \tag{6}$$

where $\left[s_1,\ s_2,\ s_3\right]$ are arbitrary constants to be determined later. Substituting Eq. (5) into Eq. (4) along (6), collecting all terms with the power of $\left[e^{-i\phi(\mathfrak{F})},\ i = 0,1,2,\dots\right]$, and equating them to zero, yield a system of algebraic equations. Solving this system we obtain

Family I

$$\left[a_1 \to \frac{a_0\left(b_1 s_1 + 2b_0 s_3\right)}{b_0 s_1}, a_2 \to \frac{2a_0 b_1 s_3}{b_0 s_1}, q_1 \to \frac{1}{2}\left(4s_2 s_3 - s_1^2\right), q_2 \to -\frac{b_0^2 s_1^2}{2a_0^2}.\right]$$

Thus, the traveling wave solutions are given in the following formula

When $(s_3 = 1)$

For $\left[s_1^2 - 4s_2 > 0\ \&\ s_2 \neq 0\right]$

$$\mathfrak{P}_1(x,t) = \frac{a_0\,e^{\imath(r_3 t + r_2(-x) + r_4)}\left(\sqrt{s_1^2 - 4s_2}\,s_1\tanh\left(\frac{1}{2}\sqrt{s_1^2 - 4s_2}\,(\eta - r_1 t + x)\right) + s_1^2 - 4s_2\right)}{b_0 s_1\left(\sqrt{s_1^2 - 4s_2}\tanh\left(\frac{1}{2}\sqrt{s_1^2 - 4s_2}\,(\eta - r_1 t + x)\right) + s_1\right)}, \tag{7}$$

$$\mathfrak{P}_2(x,t) = \frac{a_0\,e^{\imath(r_3 t + r_2(-x) + r_4)}\left(\sqrt{s_1^2 - 4s_2}\,s_1\coth\left(\frac{1}{2}\sqrt{s_1^2 - 4s_2}\,(\eta - r_1 t + x)\right) + s_1^2 - 4s_2\right)}{b_0 s_1\left(\sqrt{s_1^2 - 4s_2}\coth\left(\frac{1}{2}\sqrt{s_1^2 - 4s_2}\,(\eta - r_1 t + x)\right) + s_1\right)}. \tag{8}$$

For $\left[s_1^2 - 4s_2 > 0\ \&\ s_2 = 0\ \&\ s_1 \neq 0\right]$

$$\mathfrak{P}_3(x,t) = \frac{a_0\,e^{\imath(r_3 t + r_2(-x) + r_4)}\left(e^{s_1(\eta - r_1 t + x)} + 1\right)}{b_0\left(e^{s_1(\eta - r_1 t + x)} - 1\right)}. \tag{9}$$

For $\left[s_1^2 - 4s_2 = 0\ \&\ s_2 \neq 0\ \&\ s_1 \neq 0\right]$

$$\mathfrak{P}_4(x,t) = \frac{2a_0\,e^{\imath(r_3 t + r_2(-x) + r_4)}}{b_0\left(s_1\left(\eta - r_1 t + x\right) + 2\right)}. \tag{10}$$

For $\left[s_1^2 - 4s_2 < 0\ \&\ s_2 \neq 0\ \&\ s_1 \neq 0\right]$

$$\mathfrak{P}_5(x,t) = \frac{a_0\,e^{\imath(r_3 t + r_2(-x) + r_4)}\left(-\sqrt{4s_2 - s_1^2}\,s_1\tan\left(\frac{1}{2}\sqrt{4s_2 - s_1^2}\,(\eta - r_1 t + x)\right) + s_1^2 - 4s_2\right)}{b_0 s_1\left(s_1 - \sqrt{4s_2 - s_1^2}\tan\left(\frac{1}{2}\sqrt{4s_2 - s_1^2}\,(\eta - r_1 t + x)\right)\right)}, \tag{11}$$

$$\mathfrak{P}_6(x,t) = \frac{a_0\,e^{\imath(r_3 t + r_2(-x) + r_4)}\left(-\sqrt{4s_2 - s_1^2}\,s_1\cot\left(\frac{1}{2}\sqrt{4s_2 - s_1^2}\,(\eta - r_1 t + x)\right) + s_1^2 - 4s_2\right)}{b_0 s_1\left(s_1 - \sqrt{4s_2 - s_1^2}\cot\left(\frac{1}{2}\sqrt{4s_2 - s_1^2}\,(\eta - r_1 t + x)\right)\right)}. \tag{12}$$

Family II

$$\left[a_0 \to 0, a_2 \to \frac{2a_1 s_3}{s_1}, b_0 \to 0, q_1 \to \frac{1}{2}\left(4s_2 s_3 - s_1^2\right), q_2 \to -\frac{b_1^2 s_1^2}{2a_1^2}.\right]$$

The traveling wave solutions in this case given as

When $(s_3 = 1)$

For $\left[s_1^2 - 4s_2 > 0 \,\&\, s_2 \neq 0\right]$

$$\mathfrak{P}_7(x,t) = \frac{a_1\, e^{\iota(r_3 t + r_2(-x) + r_4)} \left(\sqrt{s_1^2 - 4s_2}\, s_1 \tanh\left(\frac{1}{2}\sqrt{s_1^2 - 4s_2}\,(\eta - r_1 t + x)\right) + s_1^2 - 4s_2\right)}{b_1 s_1 \left(\sqrt{s_1^2 - 4s_2}\tanh\left(\frac{1}{2}\sqrt{s_1^2 - 4s_2}\,(\eta - r_1 t + x)\right) + s_1\right)}, \tag{13}$$

$$\mathfrak{P}_8(x,t) = \frac{a_1\, e^{\iota(r_3 t + r_2(-x) + r_4)} \left(\sqrt{s_1^2 - 4s_2}\, s_1 \coth\left(\frac{1}{2}\sqrt{s_1^2 - 4s_2}\,(\eta - r_1 t + x)\right) + s_1^2 - 4s_2\right)}{b_1 s_1 \left(\sqrt{s_1^2 - 4s_2}\coth\left(\frac{1}{2}\sqrt{s_1^2 - 4s_2}\,(\eta - r_1 t + x)\right) + s_1\right)}. \tag{14}$$

For $\left[s_1^2 - 4s_2 > 0 \,\&\, s_2 = 0 \,\&\, s_1 \neq 0\right]$

$$\mathfrak{P}_9(x,t) = \frac{a_1\, e^{\iota(r_3 t + r_2(-x) + r_4)} \left(e^{s_1(\eta - r_1 t + x)} + 1\right)}{b_1\left(e^{s_1(\eta - r_1 t + x)} - 1\right)}. \tag{15}$$

For $\left[s_1^2 - 4s_2 = 0 \,\&\, s_2 \neq 0 \,\&\, s_1 \neq 0\right]$

$$\mathfrak{P}_{10}(x,t) = \frac{2a_1\, e^{\iota(r_3 t + r_2(-x) + r_4)}}{b_1\left(s_1(\eta - r_1 t + x) + 2\right)}. \tag{16}$$

For $\left[s_1^2 - 4s_2 < 0 \,\&\, s_2 \neq 0 \,\&\, s_1 \neq 0\right]$

$$\mathfrak{P}_{11}(x,t) = \frac{a_1\, e^{\iota(r_3 t + r_2(-x) + r_4)} \left(-\sqrt{4s_2 - s_1^2}\, s_1 \tan\left(\frac{1}{2}\sqrt{4s_2 - s_1^2}\,(\eta - r_1 t + x)\right) + s_1^2 - 4s_2\right)}{b_1 s_1 \left(s_1 - \sqrt{4s_2 - s_1^2}\tan\left(\frac{1}{2}\sqrt{4s_2 - s_1^2}\,(\eta - r_1 t + x)\right)\right)}, \tag{17}$$

$$\mathfrak{P}_{12}(x,t) = \frac{a_1\, e^{\iota(r_3 t + r_2(-x) + r_4)} \left(-\sqrt{4s_2 - s_1^2}\, s_1 \cot\left(\frac{1}{2}\sqrt{4s_2 - s_1^2}\,(\eta - r_1 t + x)\right) + s_1^2 - 4s_2\right)}{b_1 s_1 \left(s_1 - \sqrt{4s_2 - s_1^2}\cot\left(\frac{1}{2}\sqrt{4s_2 - s_1^2}\,(\eta - r_1 t + x)\right)\right)}. \tag{18}$$

Family III

$$\left[a_1 \to 0, a_2 \to -\frac{4a_0 s_3^2}{s_1^2}, b_1 \to -\frac{2b_0 s_3}{s_1}, q_1 \to \frac{1}{2}\left(4s_2 s_3 - s_1^2\right), q_2 \to -\frac{b_0^2 s_1^2}{2a_0^2}.\right]$$

then, the traveling wave solutions are given in the following formula

Case one $(s_3 = 1)$

For $\left[s_1^2 - 4s_2 > 0 \,\&\, s_2 \neq 0\right]$

$$\begin{aligned}\mathfrak{P}_{13}(x,t) = &\left(-16a_0 s_2^2\, e^{\iota(r_3 t + r_2(-x) + r_4)}\right) \Big/ \Bigg[\, b_0 s_1 \Bigg(\sqrt{s_1^2 - 4s_2} \\ &\times \tanh\left(\frac{1}{2}\sqrt{s_1^2 - 4s_2}\,(\eta - r_1 t + x)\right) + s_1\Bigg) \\ &\times \left(\sqrt{s_1^2 - 4s_2}\, s_1 \tanh\left(\frac{1}{2}\sqrt{s_1^2 - 4s_2}\,(\eta - r_1 t + x)\right) + s_1^2 + 4s_2\right)\Bigg],\end{aligned} \tag{19}$$

$$\begin{aligned}\mathfrak{P}_{14}(x,t) = &\left(-16a_0 s_2^2\, e^{\iota(r_3 t + r_2(-x) + r_4)}\right) \Big/ \Bigg[\, b_0 s_1 \Bigg(\sqrt{s_1^2 - 4s_2} \\ &\times \coth\left(\frac{1}{2}\sqrt{s_1^2 - 4s_2}\,(\eta - r_1 t + x)\right) + s_1\Bigg) \\ &\times \left(\sqrt{s_1^2 - 4s_2}\, s_1 \coth\left(\frac{1}{2}\sqrt{s_1^2 - 4s_2}\,(\eta - r_1 t + x)\right) + s_1^2 + 4s_2\right)\Bigg].\end{aligned} \tag{20}$$

For $\left[s_1^2 - 4s_2 > 0 \,\&\, s_2 = 0 \,\&\, s_1 \neq 0\right]$

$$\mathfrak{P}_{15}(x,t) = -\frac{4a_0\, e^{\iota(r_3 t + r_2(-x) + r_4)}}{b_0\left(e^{s_1(\eta - r_1 t + x)} - 3\right)\left(e^{s_1(\eta - r_1 t + x)} - 1\right)}. \tag{21}$$

For $\left[s_1^2 - 4s_2 = 0 \,\&\, s_2 \neq 0 \,\&\, s_1 \neq 0\right]$

$$\mathfrak{P}_{16}(x,t) = -\frac{a_0 s_1^2\, e^{\iota(r_3 t + r_2(-x) + r_4)}\,(\eta - r_1 t + x)^2}{b_0\left(s_1(\eta - r_1 t + x) + 2\right)\left(2s_1(\eta - r_1 t + x) + 2\right)}. \tag{22}$$

For $\left[s_1^2 - 4s_2 < 0 \,\&\, s_2 \neq 0 \,\&\, s_1 \neq 0\right]$

$$\begin{aligned}\mathfrak{P}_{17}(x,t) = &\left(-16a_0 s_2^2\, e^{\iota(r_3 t + r_2(-x) + r_4)}\right) \Big/ \Bigg[\, b_0 s_1 \Bigg(s_1 - \sqrt{4s_2 - s_1^2} \\ &\tan \times \left(\frac{1}{2}\sqrt{4s_2 - s_1^2}\,(\eta - r_1 t + x)\right)\Bigg) \\ &\times \left(-\sqrt{4s_2 - s_1^2}\, s_1 \tan\left(\frac{1}{2}\sqrt{4s_2 - s_1^2}\,(\eta - r_1 t + x)\right) + s_1^2 + 4s_2\right)\Bigg],\end{aligned} \tag{23}$$

$$\begin{aligned}\mathfrak{P}_{18}(x,t) = &\left(-16a_0 s_2^2\, e^{\iota(r_3 t + r_2(-x) + r_4)}\right) \Big/ \Bigg[\, b_0 s_1 \Bigg(s_1 - \sqrt{4s_2 - s_1^2} \\ &\times \cot\left(\frac{1}{2}\sqrt{4s_2 - s_1^2}\,(\eta - r_1 t + x)\right)\Bigg) \\ &\times \left(-\sqrt{4s_2 - s_1^2}\, s_1 \cot\left(\frac{1}{2}\sqrt{4s_2 - s_1^2}\,(\eta - r_1 t + x)\right) + s_1^2 + 4s_2\right)\Bigg].\end{aligned} \tag{24}$$

Family IV

$$\left[a_1 \to \frac{a_0 s_1}{s_2}, a_2 \to \frac{a_0 s_3}{s_2}, b_1 \to \frac{2b_0 s_3}{s_1}, q_1 \to s_1^2 - 4s_2 s_3, q_2 \to -\frac{8b_0^2 s_2^2 s_3^2}{a_0^2 s_1^2}.\right]$$

The traveling wave solutions are then

When $(s_3 = 1)$

For $\left[s_1^2 - 4s_2 > 0 \,\&\, s_2 \neq 0\right]$

$$\begin{aligned}\mathfrak{P}_{19}(x,t) = &\left(4a_0 s_1 s_2\, e^{\iota(r_3 t + r_2(-x) + r_4)}\right) \Big/ \Bigg[\, b_0 \Bigg(\sqrt{s_1^2 - 4s_2} \\ &\times \tanh\left(\frac{1}{2}\sqrt{s_1^2 - 4s_2}\,(\eta - r_1 t + x)\right) + s_1\Bigg) \\ &\times \left(\sqrt{s_1^2 - 4s_2}\, s_1 \tanh\left(\frac{1}{2}\sqrt{s_1^2 - 4s_2}\,(\eta - r_1 t + x)\right) + s_1^2 - 4s_2\right)\Bigg],\end{aligned} \tag{25}$$

$$\begin{aligned}\mathfrak{P}_{20}(x,t) = &\left(4a_0 s_1 s_2\, e^{\iota(r_3 t + r_2(-x) + r_4)}\right) \Big/ \Bigg[\, b_0 \Bigg(\sqrt{s_1^2 - 4s_2} \\ &\times \coth\left(\frac{1}{2}\sqrt{s_1^2 - 4s_2}\,(\eta - r_1 t + x)\right) + s_1\Bigg) \\ &\times \left(\sqrt{s_1^2 - 4s_2}\, s_1 \coth\left(\frac{1}{2}\sqrt{s_1^2 - 4s_2}\,(\eta - r_1 t + x)\right) + s_1^2 - 4s_2\right)\Bigg].\end{aligned} \tag{26}$$

For $\left[s_1^2-4s_2=0\,\&\,s_2\neq 0\,\&\,s_1\neq 0\right]$

$$\mathfrak{P}_{21}(x,t)=\frac{a_0 s_1^4\, e^{\iota(r_3t+r_2(-x)+r_4)}\,\left(\eta-r_1t+x\right)^2}{8b_0 s_2\left(s_1\left(\eta-r_1t+x\right)+2\right)}. \tag{27}$$

For $\left[s_1^2-4s_2<0\,\&\,s_2\neq 0\,\&\,s_1\neq 0\right]$

$$\begin{aligned}\mathfrak{P}_{22}(x,t)=&\left(4a_0s_1s_2\,e^{\iota(r_3t+r_2(-x)+r_4)}\right)\Big/\Bigg[b_0\left(s_1-\sqrt{4s_2-s_1^2}\right.\\&\left.\times\tan\left(\frac{1}{2}\sqrt{4s_2-s_1^2}\left(\eta-r_1t+x\right)\right)\right)\\&\times\left(-\sqrt{4s_2-s_1^2}s_1\tan\left(\frac{1}{2}\sqrt{4s_2-s_1^2}\left(\eta-r_1t+x\right)\right)+s_1^2-4s_2\right)\Bigg],\end{aligned} \tag{28}$$

$$\begin{aligned}\mathfrak{P}_{23}(x,t)=&\left(4a_0s_1s_2\,e^{\iota(r_3t+r_2(-x)+r_4)}\right)\Big/\Bigg[b_0\left(s_1-\sqrt{4s_2-s_1^2}\right.\\&\left.\times\cot\left(\frac{1}{2}\sqrt{4s_2-s_1^2}\left(\eta-r_1t+x\right)\right)\right)\\&\times\left(-\sqrt{4s_2-s_1^2}s_1\cot\left(\frac{1}{2}\sqrt{4s_2-s_1^2}\left(\eta-r_1t+x\right)\right)+s_1^2-4s_2\right)\Bigg].\end{aligned} \tag{29}$$

Family V

$$\Bigg[a_1\to\frac{4a_0s_3}{s_1},a_2\to\frac{4a_0s_3^2}{s_1^2},b_1\to\frac{2b_0s_3}{s_1},$$
$$q_1\to\frac{1}{2}\left(4s_2s_3-s_1^2\right),q_2\to-\frac{b_0^2s_1^2}{2a_0^2}.\Bigg]$$

The traveling wave solutions are given then

When $(s_3=1)$

For $\left[s_1^2-4s_2>0\,\&\,s_2\neq 0\right]$

$$\begin{aligned}\mathfrak{P}_{24}(x,t)=&\left(-8a_0s_2\,e^{\iota(r_3t+r_2(-x)+r_4)}\left(\sqrt{s_1^2-4s_2}s_1\right.\right.\\&\left.\left.\times\tanh\left(\frac{1}{2}\sqrt{s_1^2-4s_2}\left(\eta-r_1t+x\right)\right)+s_1^2-2s_2\right)\right)\\&\Big/\Bigg[b_0s_1\left(\sqrt{s_1^2-4s_2}\tanh\left(\frac{1}{2}\sqrt{s_1^2-4s_2}\left(\eta-r_1t+x\right)\right)\right.\\&\left.+s_1\right)\left(\sqrt{s_1^2-4s_2}s_1\right.\\&\left.\times\tanh\left(\frac{1}{2}\sqrt{s_1^2-4s_2}\left(\eta-r_1t+x\right)\right)+s_1^2-4s_2\right)\Bigg],\end{aligned} \tag{30}$$

$$\begin{aligned}\mathfrak{P}_{25}(x,t)=&\left(-8a_0s_2\,e^{\iota(r_3t+r_2(-x)+r_4)}\left(\sqrt{s_1^2-4s_2}s_1\right.\right.\\&\left.\left.\times\coth\left(\frac{1}{2}\sqrt{s_1^2-4s_2}\left(\eta-r_1t+x\right)\right)+s_1^2-2s_2\right)\right)\\&\Big/\Bigg[b_0s_1\left(\sqrt{s_1^2-4s_2}\coth\left(\frac{1}{2}\sqrt{s_1^2-4s_2}\left(\eta-r_1t+x\right)\right)+s_1\right)\\&\times\left(\sqrt{s_1^2-4s_2}s_1\coth\left(\frac{1}{2}\sqrt{s_1^2-4s_2}\left(\eta-r_1t+x\right)\right)+s_1^2-4s_2\right)\Bigg].\end{aligned} \tag{31}$$

For $\left[s_1^2-4s_2>0\,\&\,s_2=0\,\&\,s_1\neq 0\right]$

$$\begin{aligned}\mathfrak{P}_{26}(x,t)=&\frac{1}{b_0}\Bigg[2a_0\exp\left(s_1\left(\eta-r_1t+x\right)+r_3t+r_2(-x)+r_4\right)\\&\times\left(\coth\left(s_1\left(\eta-r_1t+x\right)\right)-1\right)\Bigg].\end{aligned} \tag{32}$$

For $\left[s_1^2-4s_2=0\,\&\,s_2\neq 0\,\&\,s_1\neq 0\right]$

$$\mathfrak{P}_{27}(x,t)=-\frac{a_0s_1\,e^{\iota(r_3t+r_2(-x)+r_4)}\,\left(\eta-r_1t+x\right)\left(s_1\left(\eta-r_1t+x\right)+4\right)}{2b_0\left(s_1\left(\eta-r_1t+x\right)+2\right)}. \tag{33}$$

For $\left[s_1^2-4s_2<0\,\&\,s_2\neq 0\,\&\,s_1\neq 0\right]$

$$\begin{aligned}\mathfrak{P}_{28}(x,t)=&\left(8a_0s_2\,e^{\iota(r_3t+r_2(-x)+r_4)}\left(\sqrt{4s_2-s_1^2}s_1\right.\right.\\&\left.\left.\tan\left(\frac{1}{2}\sqrt{4s_2-s_1^2}\left(\eta-r_1t+x\right)\right)-s_1^2+2s_2\right)\right)\\&\Big/\Bigg[b_0s_1\left(s_1-\sqrt{4s_2-s_1^2}\tan\left(\frac{1}{2}\sqrt{4s_2-s_1^2}\left(\eta-r_1t+x\right)\right)\right)\\&\times\left(-\sqrt{4s_2-s_1^2}s_1\tan\left(\frac{1}{2}\sqrt{4s_2-s_1^2}\left(\eta-r_1t+x\right)\right)+s_1^2-4s_2\right)\Bigg],\end{aligned} \tag{34}$$

$$\begin{aligned}\mathfrak{P}_{29}(x,t)=&\left(8a_0s_2\,e^{\iota(r_3t+r_2(-x)+r_4)}\left(\sqrt{4s_2-s_1^2}s_1\right.\right.\\&\left.\left.\times\cot\left(\frac{1}{2}\sqrt{4s_2-s_1^2}\left(\eta-r_1t+x\right)\right)-s_1^2+2s_2\right)\right)\\&\Big/\Bigg[b_0s_1\left(s_1-\sqrt{4s_2-s_1^2}\cot\left(\frac{1}{2}\sqrt{4s_2-s_1^2}\left(\eta-r_1t+x\right)\right)\right)\\&\times\left(-\sqrt{4s_2-s_1^2}s_1\cot\left(\frac{1}{2}\sqrt{4s_2-s_1^2}\left(\eta-r_1t+x\right)\right)+s_1^2-4s_2\right)\Bigg].\end{aligned} \tag{35}$$

Family VI

$$\Bigg[a_1\to\frac{2a_0s_1s_3}{s_1^2-2s_2s_3},a_2\to-\frac{2a_0s_3^2}{2s_2s_3-s_1^2},b_1\to\frac{2b_0s_3}{s_1},$$
$$q_1\to-2\left(s_1^2-4s_2s_3\right),q_2\to-\frac{2b_0^2\left(s_1^2-2s_2s_3\right)^2}{a_0^2s_1^2}.\Bigg]$$

The traveling wave solutions are then

When $(s_3=1)$

For $\left[s_1^2-4s_2>0\,\&\,s_2\neq 0\right]$

$$\mathfrak{P}_{30}(x,t)=\frac{a_0\,e^{\iota(r_3t+r_2(-x)+r_4)}\left(1-\frac{4s_2\left(\sqrt{s_1^2-4s_2}s_1\tanh\left(\frac{1}{2}\sqrt{s_1^2-4s_2}(\eta-r_1t+x)\right)+s_1^2-2s_2\right)}{\left(s_1^2-2s_2\right)\left(\sqrt{s_1^2-4s_2}\tanh\left(\frac{1}{2}\sqrt{s_1^2-4s_2}(\eta-r_1t+x)\right)+s_1\right)^2}\right)}{b_0\left(1-\frac{4s_2}{\sqrt{s_1^2-4s_2}s_1\tanh\left(\frac{1}{2}\sqrt{s_1^2-4s_2}(\eta-r_1t+x)\right)+s_1^2}\right)}, \tag{36}$$

$$\mathfrak{P}_{31}(x,t)=\frac{a_0\,e^{\iota(r_3t+r_2(-x)+r_4)}\left(1-\frac{4s_2\left(\sqrt{s_1^2-4s_2}s_1\coth\left(\frac{1}{2}\sqrt{s_1^2-4s_2}(\eta-r_1t+x)\right)+s_1^2-2s_2\right)}{\left(s_1^2-2s_2\right)\left(\sqrt{s_1^2-4s_2}\coth\left(\frac{1}{2}\sqrt{s_1^2-4s_2}(\eta-r_1t+x)\right)+s_1\right)^2}\right)}{b_0\left(1-\frac{4s_2}{\sqrt{s_1^2-4s_2}s_1\coth\left(\frac{1}{2}\sqrt{s_1^2-4s_2}(\eta-r_1t+x)\right)+s_1^2}\right)}. \tag{37}$$

For $\left[s_1^2-4s_2>0\,\&\,s_2=0\,\&\,s_1\neq 0\right]$

$$\mathfrak{P}_{32}(x,t)=\frac{1}{b_0}\left(a_0\,e^{\iota(r_3t+r_2(-x)+r_4)}\coth\left(s_1\left(\eta-r_1t+x\right)\right)\right). \tag{38}$$

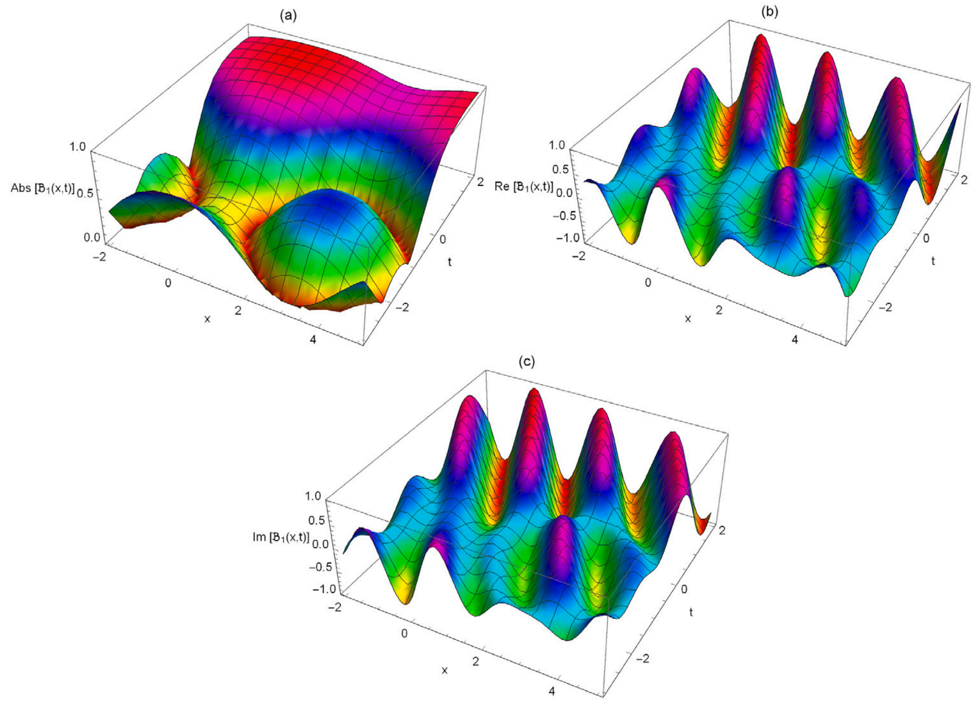

Fig. 1. Numerical simulation of absolute, real, and imaginary Eq. (7) in three-dimensional plots.

For $\left[s_1^2 - 4s_2 = 0 \,\&\, s_2 \neq 0 \,\&\, s_1 \neq 0\right]$

$$\begin{aligned}\mathfrak{P}_{33}(x,t) =& \frac{1}{4b_0}\left[a_0\, e^{t\,(r_3 t + r_2(-x)+r_4)}\, \left(s_1\left(\eta - r_1 t + x\right)+2\right)\right. \\ & \left.\times\left(2 - \frac{s_1^3\left(\eta - r_1 t + x\right)\left(s_1\left(\eta - r_1 t + x\right)+4\right)}{\left(s_1^2 - 2s_2\right)\left(s_1\left(\eta - r_1 t + x\right)+2\right)^2}\right)\right].\end{aligned} \tag{39}$$

For $\left[s_1^2 - 4s_2 < 0 \,\&\, s_2 \neq 0 \,\&\, s_1 \neq 0\right]$

$$\mathfrak{P}_{34}(x,t) = \frac{a_0\, e^{t\,(r_3 t + r_2(-x)+r_4)}\left(\frac{4s_2\left(\sqrt{4s_2-s_1^2}\,s_1 \tan\left(\frac{1}{2}\sqrt{4s_2-s_1^2}(\eta-r_1t+x)\right)-s_1^2+2s_2\right)}{\left(s_1^2-2s_2\right)\left(s_1-\sqrt{4s_2-s_1^2}\tan\left(\frac{1}{2}\sqrt{4s_2-s_1^2}(\eta-r_1t+x)\right)\right)^2}+1\right)}{b_0\left(1-\frac{4s_2}{s_1^2-s_1\sqrt{4s_2-s_1^2}\tan\left(\frac{1}{2}\sqrt{4s_2-s_1^2}(\eta-r_1t+x)\right)}\right)}, \tag{40}$$

$$\mathfrak{P}_{35}(x,t) = \frac{a_0\, e^{t\,(r_3 t + r_2(-x)+r_4)}\left(\frac{4s_2\left(\sqrt{4s_2-s_1^2}\,s_1 \cot\left(\frac{1}{2}\sqrt{4s_2-s_1^2}(\eta-r_1t+x)\right)-s_1^2+2s_2\right)}{\left(s_1^2-2s_2\right)\left(s_1-\sqrt{4s_2-s_1^2}\cot\left(\frac{1}{2}\sqrt{4s_2-s_1^2}(\eta-r_1t+x)\right)\right)^2}+1\right)}{b_0\left(1-\frac{4s_2}{s_1^2-s_1\sqrt{4s_2-s_1^2}\cot\left(\frac{1}{2}\sqrt{4s_2-s_1^2}(\eta-r_1t+x)\right)}\right)}. \tag{41}$$

***Note that,* when $\left(s_1 = 1\right)$ and $\left(s_2 = s_1 = 0\right)$ for all above families $\left[\text{I, II, III, IV, V, VI}\right]$, we get a trivial solutions.**

2.2. The generalized Kudryashov method

By applying the generalized Kudryashov method, in Eq. (1) we construct the general solution of Eq. (4) as:

$$Y(\mathfrak{F}) = \frac{\sum_{i=0}^{m} a_i\, Q(\mathfrak{F})^i}{\sum_{j=0}^{n} b_j\, \mathfrak{Q}(\mathfrak{F})^j} = \frac{a_2\, \mathfrak{Q}(\mathfrak{F})^2 + a_1\, \mathfrak{Q}(\mathfrak{F}) + a_0}{b_1\, \mathfrak{Q}(\mathfrak{F}) + b_0}, \tag{42}$$

where $\left[a_0, a_1, a_2, b_0, b_1\right]$ are arbitrary constants. Also, $\mathfrak{Q}(\mathfrak{F})$ is the solution function of the following ordinary differential equation

$$\mathfrak{Q}'(\mathfrak{F}) = \mathfrak{Q}(\mathfrak{F})^2 - \mathfrak{Q}(\mathfrak{F}), \tag{43}$$

Substituting Eq. (42) into Eq. (4) along (43), collecting all terms with the power of $\left[\mathfrak{Q}(\mathfrak{F})^i,\ i = 0, 1, 2, \ldots\right]$, and equating them to zero, yield a system of algebraic equations. Their solutions are given as following:

Family I

$$\left[a_0 \to \frac{a_1 b_0}{b_1 - 2b_0}, a_2 \to -\frac{2a_1 b_1}{b_1 - 2b_0}, q_1 \to -\frac{1}{2}, q_2 \to -\frac{\left(b_1 - 2b_0\right)^2}{2a_1^2}.\right]$$

Family II

$$\left[a_0 \to -\frac{a_1}{2}, a_2 \to -a_1, b_1 \to -2b_0, q_1 \to -2, q_2 \to -\frac{8b_0^2}{a_1^2}.\right]$$

Family III

$$\left[a_0 \to -\frac{a_1}{4}, a_2 \to -a_1, b_1 \to -2b_0, q_1 \to -\frac{1}{2}, q_2 \to -\frac{8b_0^2}{a_1^2}.\right]$$

Family IV

$$\left[a_1 \to 0, a_2 \to -4a_0, b_1 \to 2b_0, q_1 \to -\frac{1}{2}, q_2 \to -\frac{b_0^2}{2a_0^2}.\right]$$

Family V

$$\left[a_0 \to \frac{ib_0}{\sqrt{2}\sqrt{q_2}}, a_1 \to \frac{i\left(b_1 - 2b_0\right)}{\sqrt{2}\sqrt{q_2}}, a_2 \to -\frac{i\sqrt{2}b_1}{\sqrt{q_2}}, q_1 \to -\frac{1}{2}.\right]$$

Family VI

$$\left[a_0 \to 0, a_1 \to -\frac{ib_1}{\sqrt{2}\sqrt{q_2}}, a_2 \to \frac{i\sqrt{2}b_1}{\sqrt{q_2}}, b_0 \to 0, q_1 \to -\frac{1}{2}.\right]$$

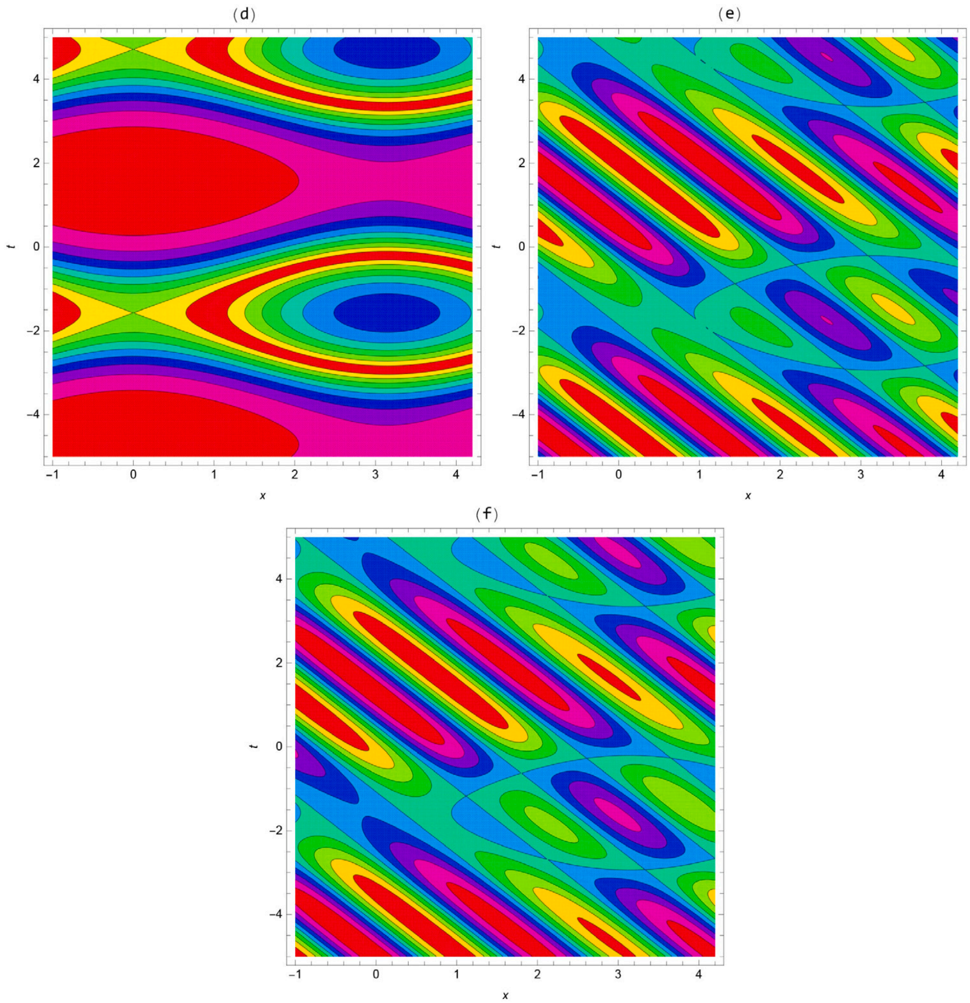

Fig. 2. Numerical simulation of absolute, real, and imaginary Eq. (7) in contour plots.

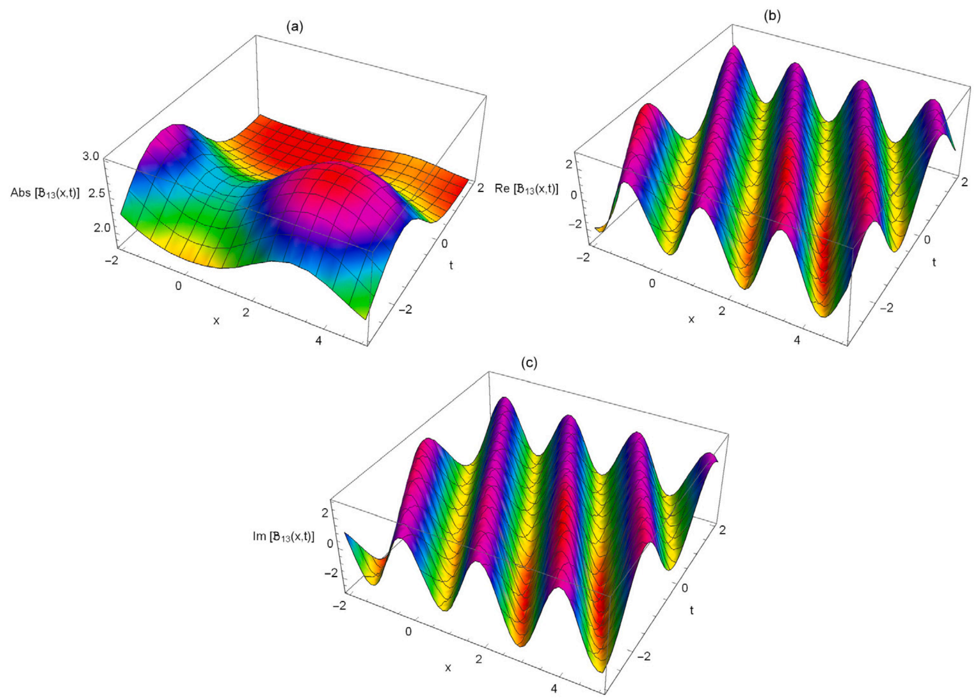

Fig. 3. Numerical simulation of absolute, real, and imaginary Eq. (19) in three-dimensional plots.

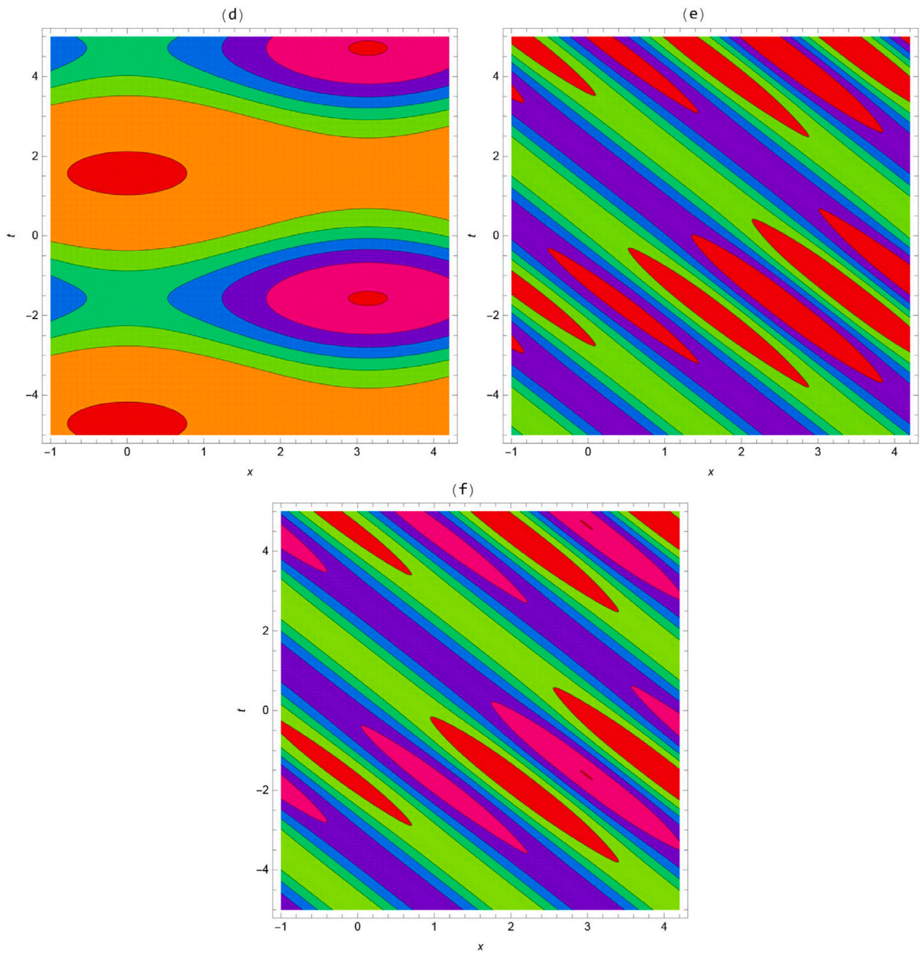

Fig. 4. Numerical simulation of absolute, real, and imaginary Eq. (19) in contour plots.

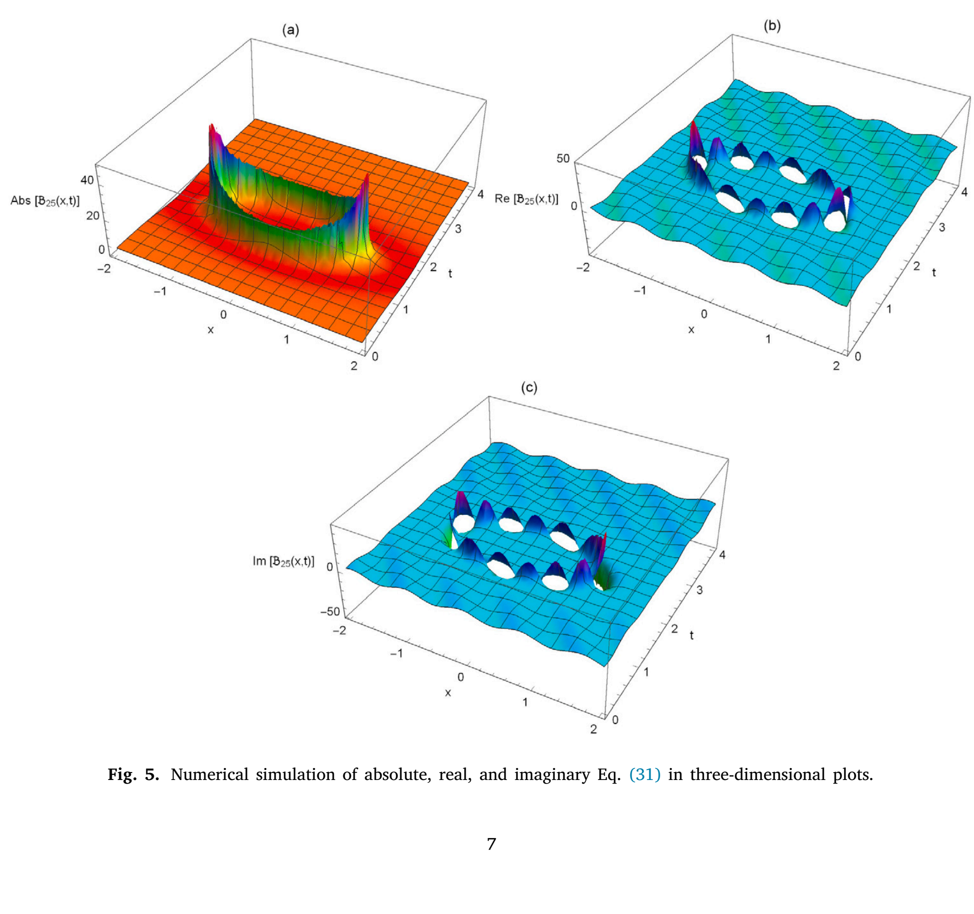

Fig. 5. Numerical simulation of absolute, real, and imaginary Eq. (31) in three-dimensional plots.

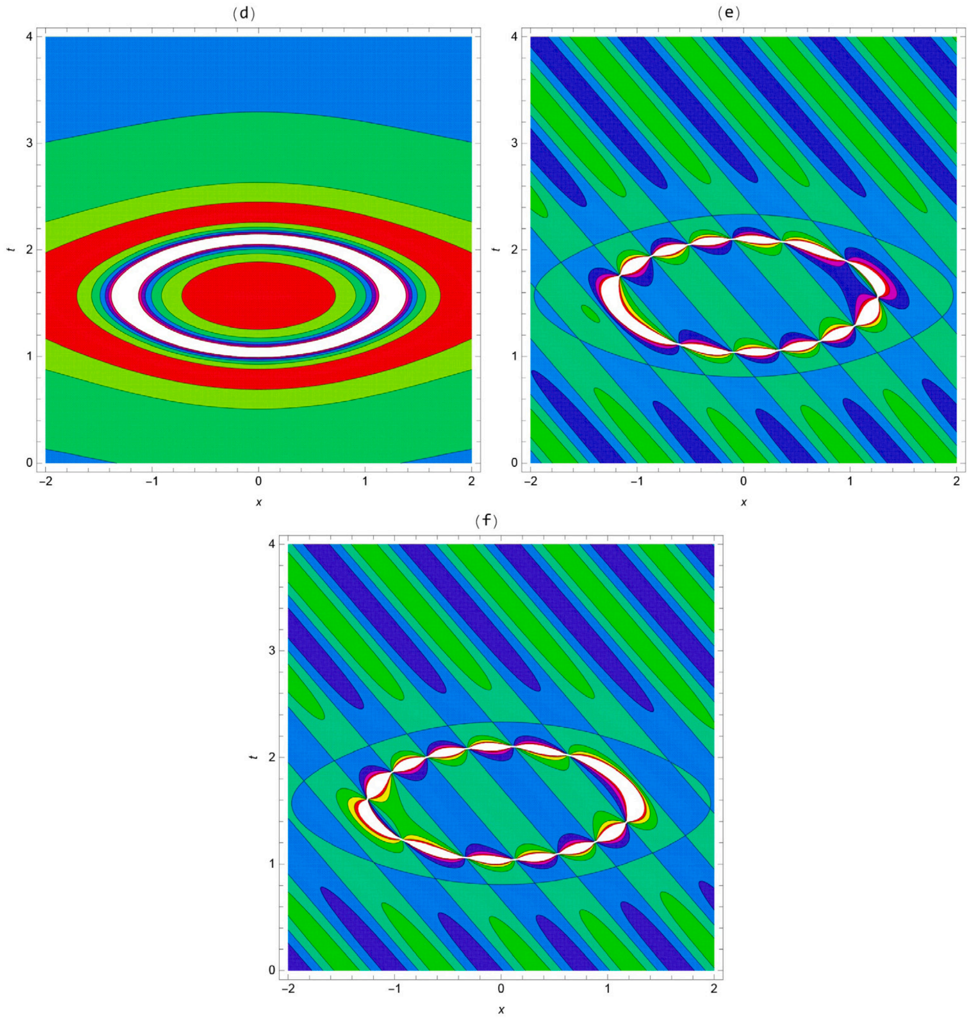

Fig. 6. Numerical simulation of absolute, real, and imaginary Eq. (31) in contour plots.

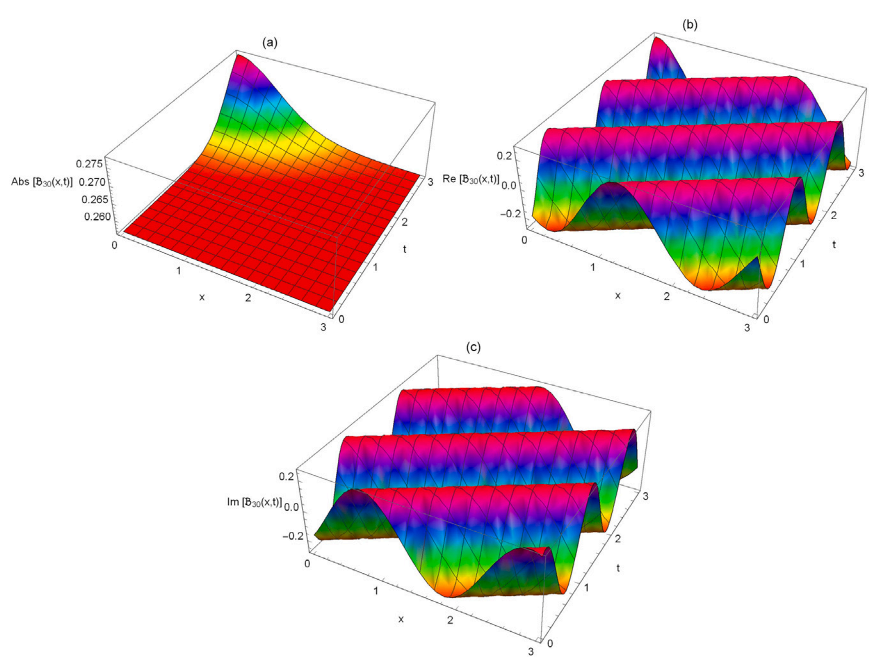

Fig. 7. Numerical simulation of absolute, real, and imaginary Eq. (36) in three-dimensional plots.

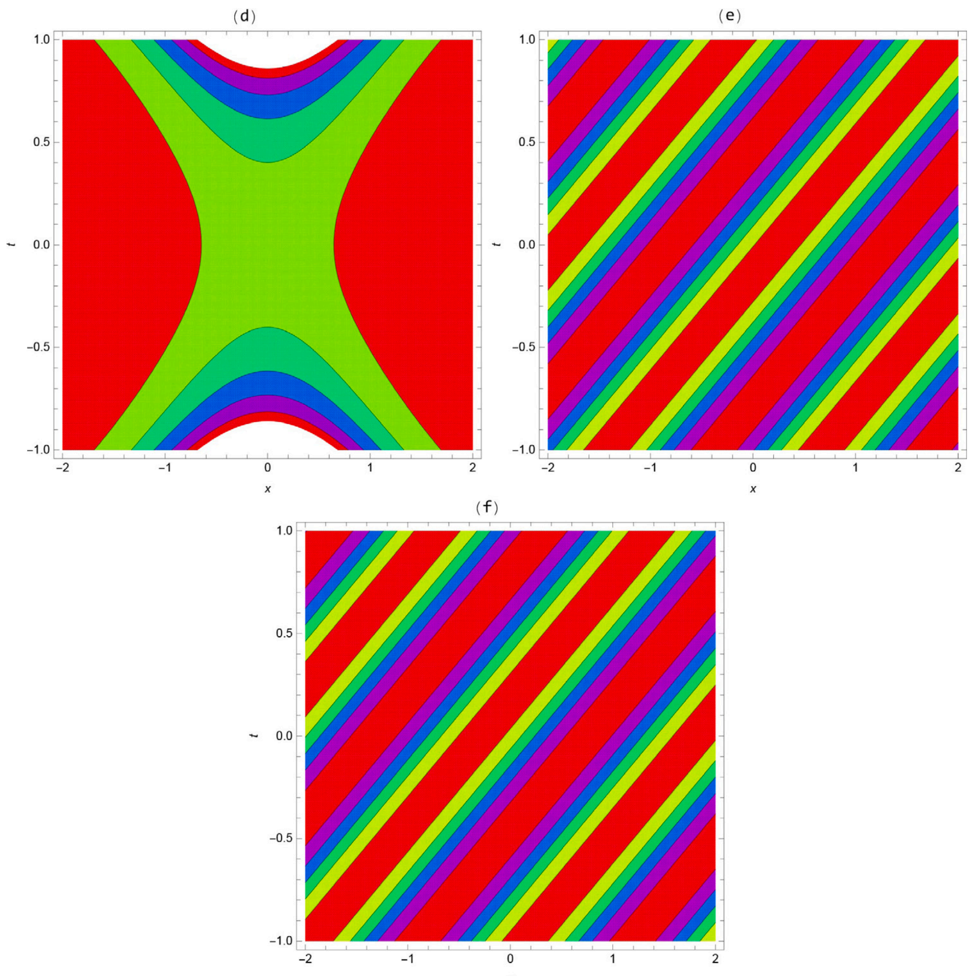

Fig. 8. Numerical simulation of absolute, real, and imaginary Eq. (36) in contour plot plots.

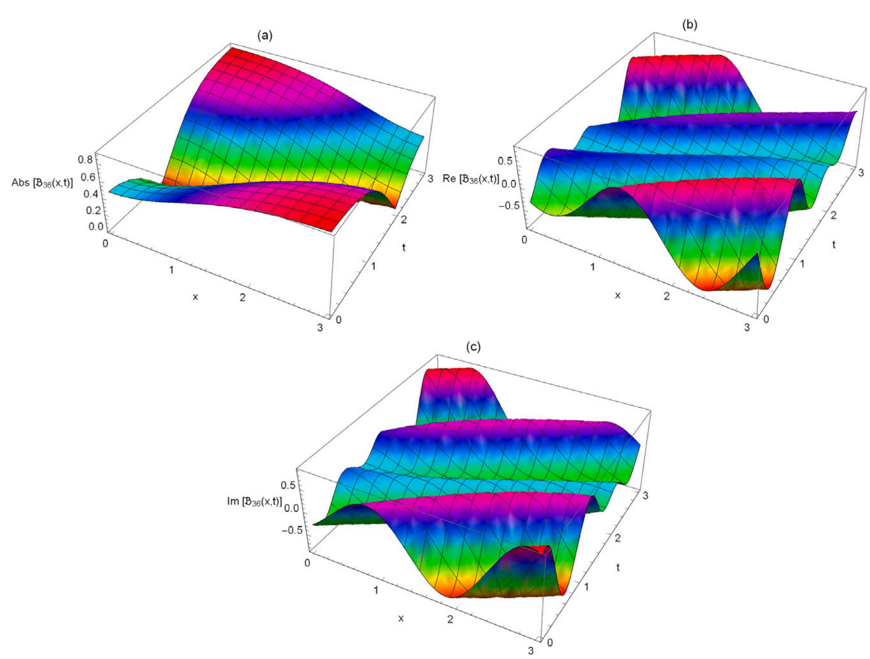

Fig. 9. Numerical simulation of absolute, real, and imaginary Eq. (44) in three-dimensional plots.

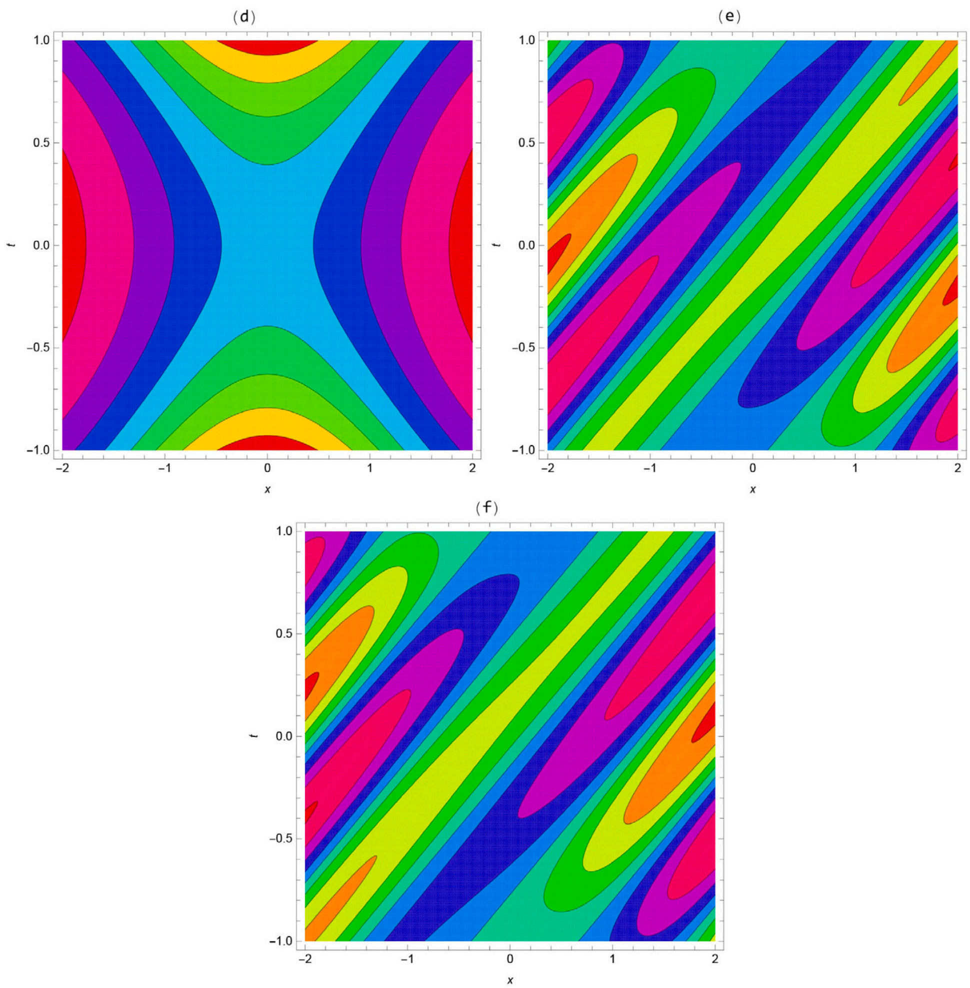

Fig. 10. Numerical simulation of absolute, real, and imaginary Eq. (44) in contour plots.

Family VII

$$\left[a_0 \to 0, a_1 \to -\frac{2i\sqrt{2}b_0}{\sqrt{q_2}}, a_2 \to \frac{2i\sqrt{2}b_0}{\sqrt{q_2}}, b_1 \to -2b_0, q_1 \to 1.\right]$$

Family VIII

$$\left[a_0 \to \frac{i\sqrt{2}b_0}{\sqrt{q_2}}, a_1 \to -\frac{2i\sqrt{2}b_0}{\sqrt{q_2}}, a_2 \to \frac{2i\sqrt{2}b_0}{\sqrt{q_2}}, b_1 \to -2b_0, q_1 \to -2.\right]$$

Family IX

$$\left[a_0 \to \frac{ib_0}{\sqrt{2}\sqrt{q_2}}, a_1 \to 0, a_2 \to -\frac{2i\sqrt{2}b_0}{\sqrt{q_2}}, b_1 \to 2b_0, q_1 \to -\frac{1}{2}.\right]$$

Thus, the traveling wave solutions are respectively given in the following formulas

$$\mathfrak{P}_{36}(x,t) = \frac{a_1 e^{i(r_3 t + r_2(-x) + r_4)}\left(e^{r_1 t} - Ae^{x}\right)}{\left(2b_0 - b_1\right)\left(Ae^{x} + e^{r_1 t}\right)}. \tag{44}$$

$$\mathfrak{P}_{37}(x,t) = \frac{a_1 e^{i(r_3 t + r_2(-x) + r_4)}\left(A^2 e^{2x} + e^{2r_1 t}\right)}{2b_0\left(e^{2r_1 t} - A^2 e^{2x}\right)}. \tag{45}$$

$$\mathfrak{P}_{38}(x,t) = \frac{a_1 e^{i(r_3 t + r_2(-x) + r_4)}\left(e^{r_1 t} - Ae^{x}\right)}{4b_0\left(Ae^{x} + e^{r_1 t}\right)}. \tag{46}$$

$$\mathfrak{P}_{39}(x,t) = -\frac{a_0 e^{i(r_3 t + r_2(-x) + r_4)}\left(e^{r_1 t} - Ae^{x}\right)}{b_0\left(Ae^{x} + e^{r_1 t}\right)}. \tag{47}$$

$$\mathfrak{P}_{40}(x,t) = -\frac{i e^{i(r_3 t + r_2(-x) + r_4)}\left(e^{r_1 t} - Ae^{x}\right)}{\sqrt{2}\sqrt{q_2}\left(Ae^{x} + e^{r_1 t}\right)}. \tag{48}$$

$$\mathfrak{P}_{41}(x,t) = \frac{i e^{i(r_3 t + r_2(-x) + r_4)}\left(e^{r_1 t} - Ae^{x}\right)}{\sqrt{2}\sqrt{q_2}\left(Ae^{x} + e^{r_1 t}\right)}. \tag{49}$$

$$\mathfrak{P}_{42}(x,t) = \frac{2i\sqrt{2}Ae^{r_1 t + ir_3 t - ir_2 x + ir_4 + x}}{\sqrt{q_2}\left(e^{2r_1 t} - A^2 e^{2x}\right)}. \tag{50}$$

$$\mathfrak{P}_{43}(x,t) = -\frac{i\sqrt{2}e^{i(r_3 t + r_2(-x) + r_4)}\left(A^2 e^{2x} + e^{2r_1 t}\right)}{\sqrt{q_2}\left(e^{2r_1 t} - A^2 e^{2x}\right)}. \tag{51}$$

$$\mathfrak{P}_{45}(x,t) = -\frac{i e^{i(r_3 t + r_2(-x) + r_4)}\left(e^{r_1 t} - Ae^{x}\right)}{\sqrt{2}\sqrt{q_2}\left(Ae^{x} + e^{r_1 t}\right)}. \tag{52}$$

2.3. The modified Khater method

Handling Eq. (1) by applying the modified Khater method, we obtain the general solution of Eq. (4) in the following formula

$$Y(\mathfrak{F}) = \sum_{i=1}^{n} a_i\, \Gamma^{i\,\mathfrak{I}(\mathfrak{F})} + \sum_{i=1}^{n} b_i\, \Gamma^{-i\,\mathfrak{I}(\mathfrak{F})} + a_0 = a_1\, \Gamma^{\mathfrak{I}(\mathfrak{F})} + a_0 + b_1\, \Gamma^{-\mathfrak{I}(\mathfrak{F})}, \tag{53}$$

where $\left[a_0,\, a_1,\, b_1,\, \Gamma\left(\Gamma \neq 0,\, \Gamma \neq 1\right)\right]$ are arbitrary constants. Also, $\mathfrak{I}(\mathfrak{F})$ is the solution function of the following ordinary differential equation

$$\mathfrak{I}'(\mathfrak{F}) = \frac{1}{\ln(\Gamma)}\left[v_3\, \Gamma^{\mathfrak{I}(\mathfrak{F})} + v_1\, \Gamma^{-\mathfrak{I}(\mathfrak{F})} + v_2\right], \tag{54}$$

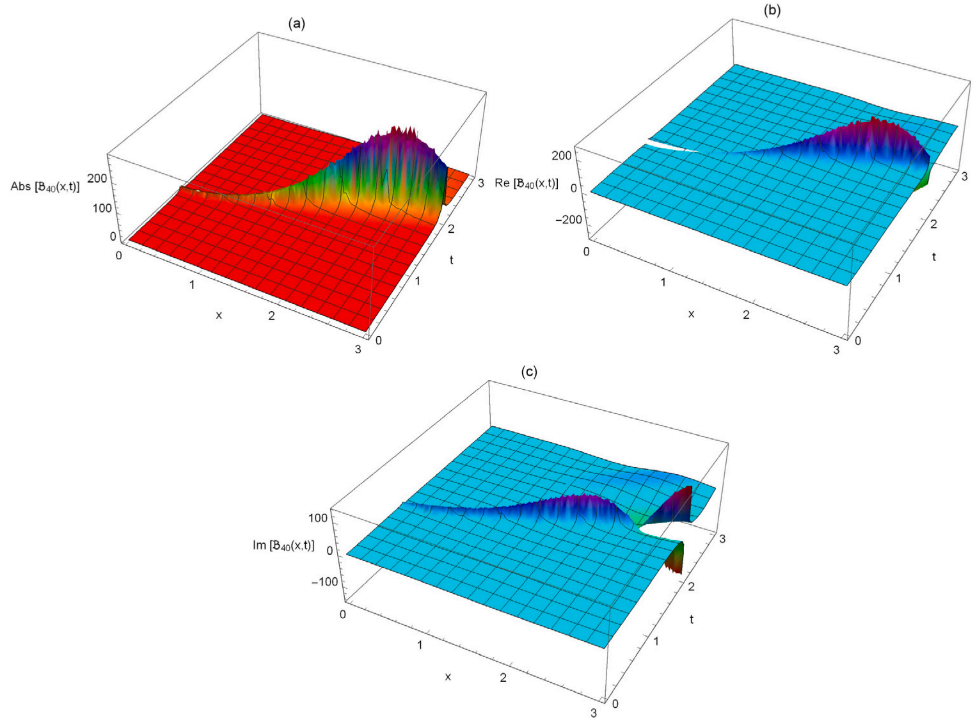

Fig. 11. Numerical simulation of absolute, real, and imaginary Eq. (48) in three-dimensional plots.

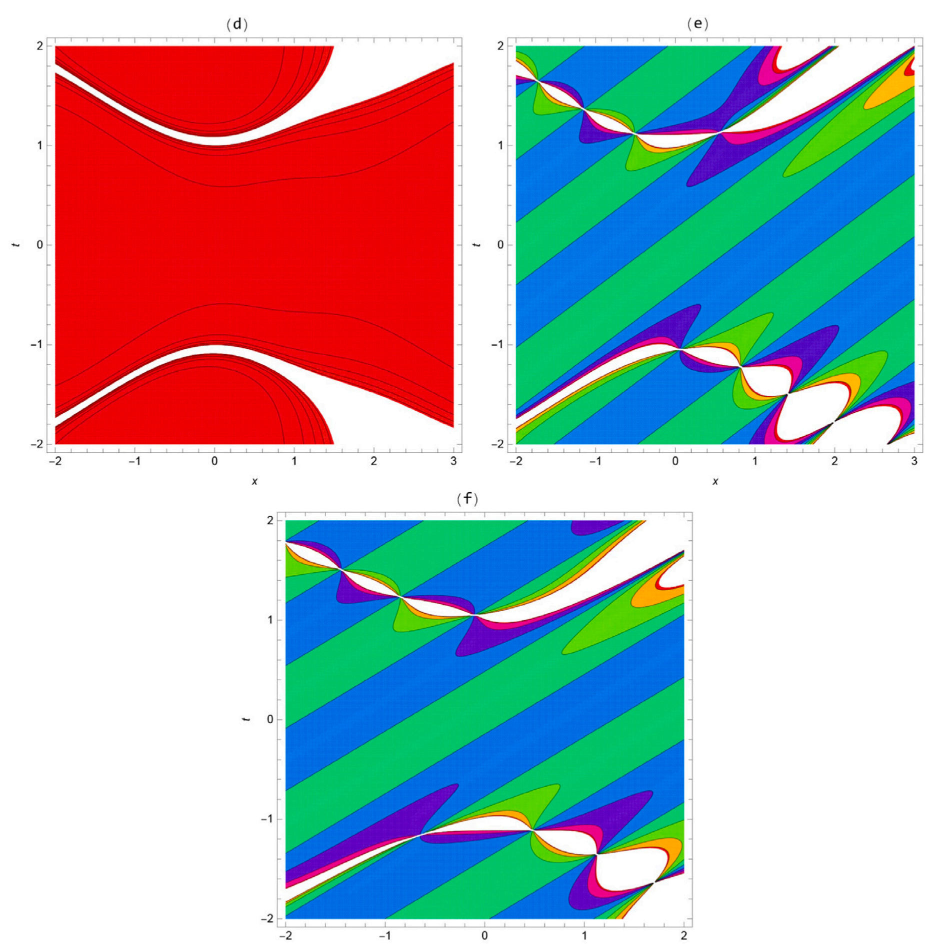

Fig. 12. Numerical simulation of absolute, real, and imaginary Eq. (48) in contour plots.

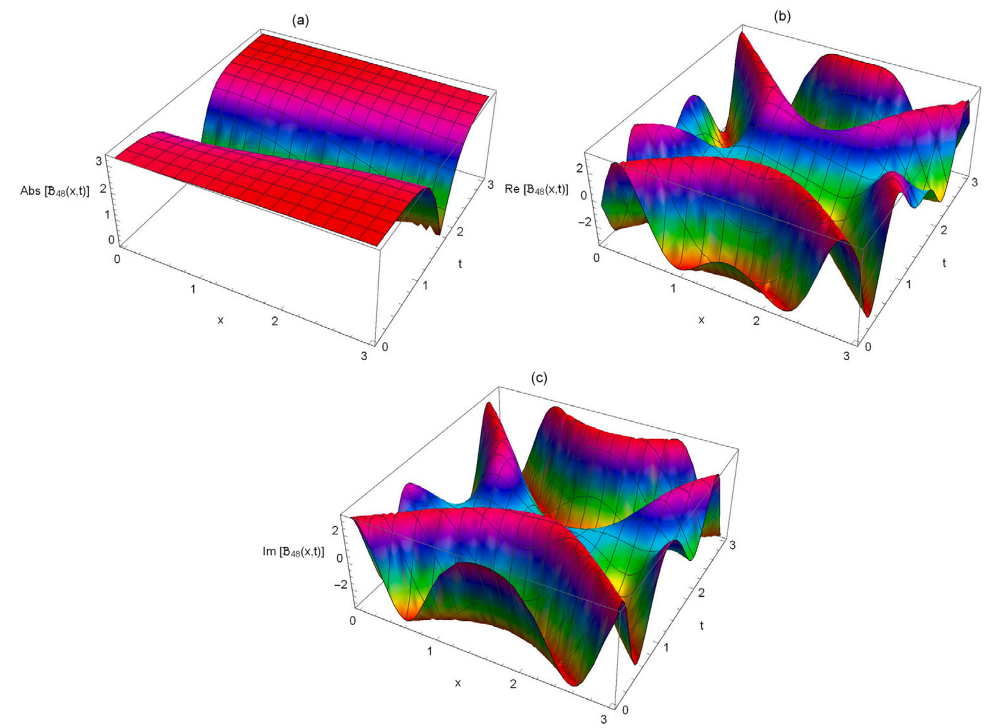

Fig. 13. Numerical simulation of absolute, real, and imaginary Eq. (57) in three-dimensional plots.

where $\left[v_1,\, v_2,\, v_3\right]$ are arbitrary constants to be determined later. Substituting Eq. (53) into Eq. (4) along (54), collecting all terms with the power of $\left[\Gamma^{i\,\mathfrak{F}(\mathfrak{F})},\ i = 0, 1, 2, \ldots\right]$, and equating them to zero, yield a system of algebraic equations. Solving this system we get

Family I

$$\left[a_1 \to \frac{2a_0 v_3}{v_2}, b_1 \to 0, q_1 \to \frac{1}{2}\left(4v_3 v_1 - v_2^2\right), q_2 \to -\frac{v_2^2}{2a_0^2}.\right]$$

Thus, the traveling wave solutions are given in the following formulas

For $\left[v_2^2 - 4v_1 v_3 < 0 \,\&\, v_3 \neq 0\right]$

$$\mathfrak{P}_{46}(x,t) = \frac{1}{v_2}\left(a_0\sqrt{4v_1v_3 - v_2^2}\, e^{\iota(r_3 t + r_2(-x) + r_4)} \tan\left(\frac{1}{2}\sqrt{4v_1v_3 - v_2^2}\left(x - r_1 t\right)\right)\right), \tag{55}$$

$$\mathfrak{P}_{47}(x,t) = \frac{1}{v_2}\left(a_0\sqrt{4v_1v_3 - v_2^2}\, e^{\iota(r_3 t + r_2(-x) + r_4)} \cot\left(\frac{1}{2}\sqrt{4v_1v_3 - v_2^2}\left(x - r_1 t\right)\right)\right). \tag{56}$$

For $\left[v_2^2 - 4v_1 v_3 < 0 \,\&\, v_3 \neq 0\right]$

$$\mathfrak{P}_{48}(x,t) = \frac{-1}{v_2}\left(a_0\sqrt{v_2^2 - 4v_1v_3}\, e^{\iota(r_3 t + r_2(-x) + r_4)} \tanh\left(\frac{1}{2}\sqrt{v_2^2 - 4v_1v_3}\left(x - r_1 t\right)\right)\right), \tag{57}$$

$$\mathfrak{P}_{49}(x,t) = \frac{-1}{v_2}\left(a_0\sqrt{v_2^2 - 4v_1v_3}\, e^{\iota(r_3 t + r_2(-x) + r_4)} \coth\left(\frac{1}{2}\sqrt{v_2^2 - 4v_1v_3}\left(x - r_1 t\right)\right)\right). \tag{58}$$

For $\left[v_2 = v_3 = \kappa \,\&\, v_1 = 0\right]$

$$\mathfrak{P}_{50}(x,t) = a_0\left(-e^{\iota(r_3 t + r_2(-x) + r_4)}\right)\coth\left(\frac{1}{2}\kappa\left(x - r_1 t\right)\right). \tag{59}$$

For $\left[v_1 = 0 \,\&\, v_2 \neq 0 \,\&\, v_3 \neq 0\right]$

$$\mathfrak{P}_{51}(x,t) = -\frac{a_0\, e^{\iota(r_3 t + r_2(-x) + r_4)}\left(v_3 e^{v_2(x - r_1 t)} + 2\right)}{v_3 e^{v_2(x - r_1 t)} - 2}. \tag{60}$$

Family II

$$\left[a_1 \to 0, b_1 \to \frac{2a_0 v_1}{v_2}, q_1 \to \frac{1}{2}\left(4v_3 v_1 - v_2^2\right), q_2 \to -\frac{v_2^2}{2a_0^2}.\right]$$

Thus, the traveling wave solutions are given in the following formulas

For $\left[v_2^2 - 4v_1 v_3 < 0 \,\&\, v_3 \neq 0\right]$

$$\mathfrak{P}_{52}(x,t) = a_0\, e^{\iota(r_3 t + r_2(-x) + r_4)} \times\left(1 - \frac{4v_1 v_3}{v_2^2 - v_2\sqrt{4v_1v_3 - v_2^2}\tan\left(\frac{1}{2}\sqrt{4v_1v_3 - v_2^2}\left(x - r_1 t\right)\right)}\right), \tag{61}$$

$$\mathfrak{P}_{53}(x,t) = a_0\, e^{\iota(r_3 t + r_2(-x) + r_4)} \times\left(1 - \frac{4v_1 v_3}{v_2^2 - v_2\sqrt{4v_1v_3 - v_2^2}\cot\left(\frac{1}{2}\sqrt{4v_1v_3 - v_2^2}\left(x - r_1 t\right)\right)}\right). \tag{62}$$

For $\left[v_2^2 - 4v_1 v_3 < 0 \,\&\, v_3 \neq 0\right]$

$$\mathfrak{P}_{54}(x,t) = a_0\, e^{\iota(r_3 t + r_2(-x) + r_4)} \times\left(1 - \frac{4v_1 v_3}{\sqrt{v_2^2 - 4v_1v_3}\,v_2\tanh\left(\frac{1}{2}\sqrt{v_2^2 - 4v_1v_3}\left(x - r_1 t\right)\right) + v_2^2}\right), \tag{63}$$

$$\mathfrak{P}_{55}(x,t) = a_0\, e^{\iota(r_3 t + r_2(-x) + r_4)}$$

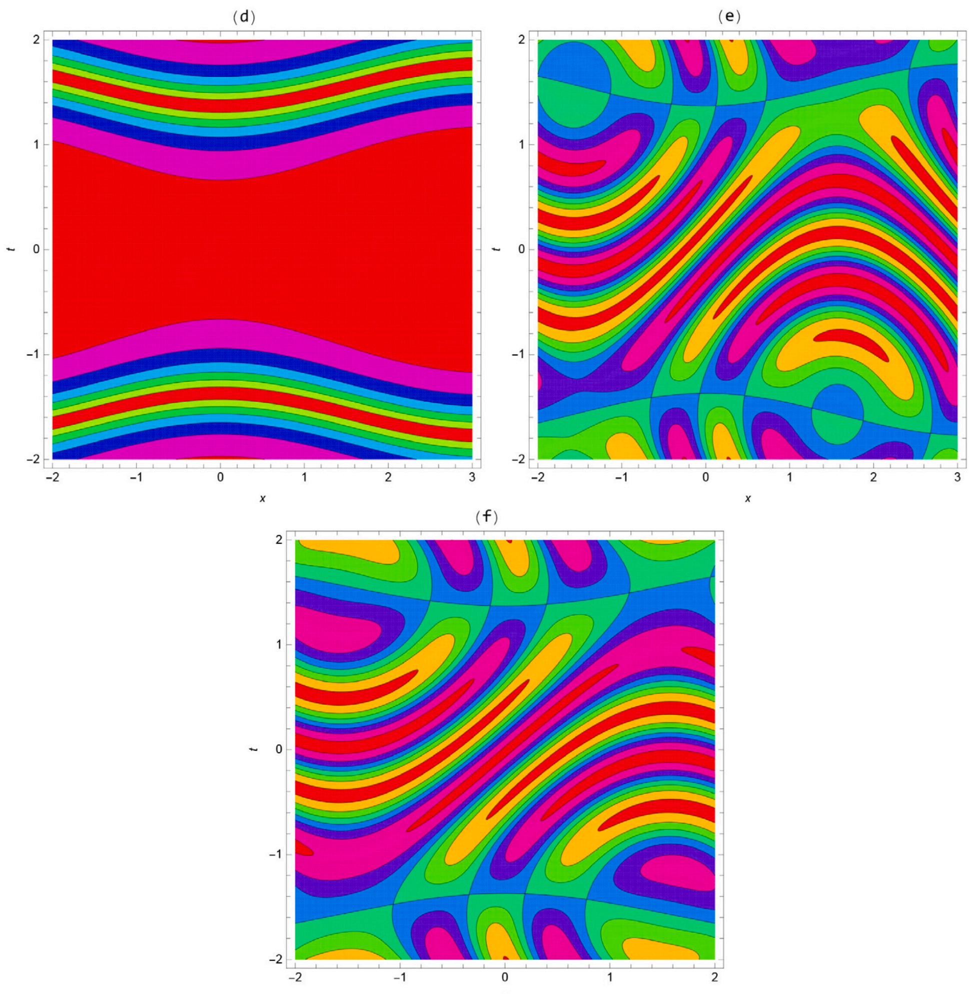

Fig. 14. Numerical simulation of absolute, real, and imaginary Eq. (57) in contour plots.

$$\times\left(1-\frac{4v_1v_3}{\sqrt{v_2^2-4v_1v_3}v_2\coth\left(\frac{1}{2}\sqrt{v_2^2-4v_1v_3}\left(x-r_1t\right)\right)+v_2^2}\right). \quad (64)$$

For $\left[v_2=\frac{v_1}{2}=\kappa\,\&\,v_3=0\right]$

$$\mathfrak{P}_{56}(x,t)=a_0\,e^{\iota(r_3t+r_2(-x)+r_4)}\left(\frac{4}{e^{\kappa(x-r_1t)}-2}+1\right). \quad (65)$$

For $\left[v_3=0\,\&\,v_2\neq 0\,\&\,v_1\neq 0\right]$

$$\mathfrak{P}_{57}(x,t)=a_0\,e^{\iota(r_3t+r_2(-x)+r_4)}\left(1-\frac{2v_1}{v_1-v_2e^{v_2(x-r_1t)}}\right). \quad (66)$$

3. Stability

In this section, we will explore the stability property of the obtained solutions using the Hamiltonian method for the dimensionless version of the Zakharov (ZE) equation. The momentum is given by the following formula:

$$\mathcal{E}=\frac{1}{2}\int_{-\mathcal{G}}^{\mathcal{G}}Y^2(\mathfrak{F})\,d\,\mathfrak{F}, \quad (67)$$

where $\mathcal{G}$, $-\mathcal{G}$ are arbitrary constants. Thus, the condition for stability is given in the next condition:

$$\left.\frac{\partial\mathcal{E}}{\partial r_1}\right|_{r_1=\mathfrak{K}}>0. \quad (68)$$

where r_1, $\mathfrak{K}$ are arbitrary constants.

Investigating the stability of the solution of Eq. (4) by using (7) with the following values of the constants $\left[a_0=5,\ b_0=6,\ \eta=4,\ s_1=3,\ s_2=2\right]$, yields:

$$\mathcal{E}=\frac{1}{162r_1}\Big[25\left(25r_1-\log\left(e^{-5r_1}+2e^9\right)+\log\left(e^{5r_1}+2e^9\right)\right. \\ \left.-\log\left(e^{5r_1+1}+2\right)+\log\left(e^{1-5r_1}+2\right)\right)\Big] \quad (69)$$

Thus,

$$\left.\frac{\partial\mathcal{E}}{\partial r_1}\right|_{r_1=2}=0.2009804350>0. \quad (70)$$

This means, that this solution is stable.

Investigating the stability of the solution of Eq. (4) by using (44) with the following values of the constants $\Big[b_1=3,\ a_1=4,\ A=5,\ b_0=$

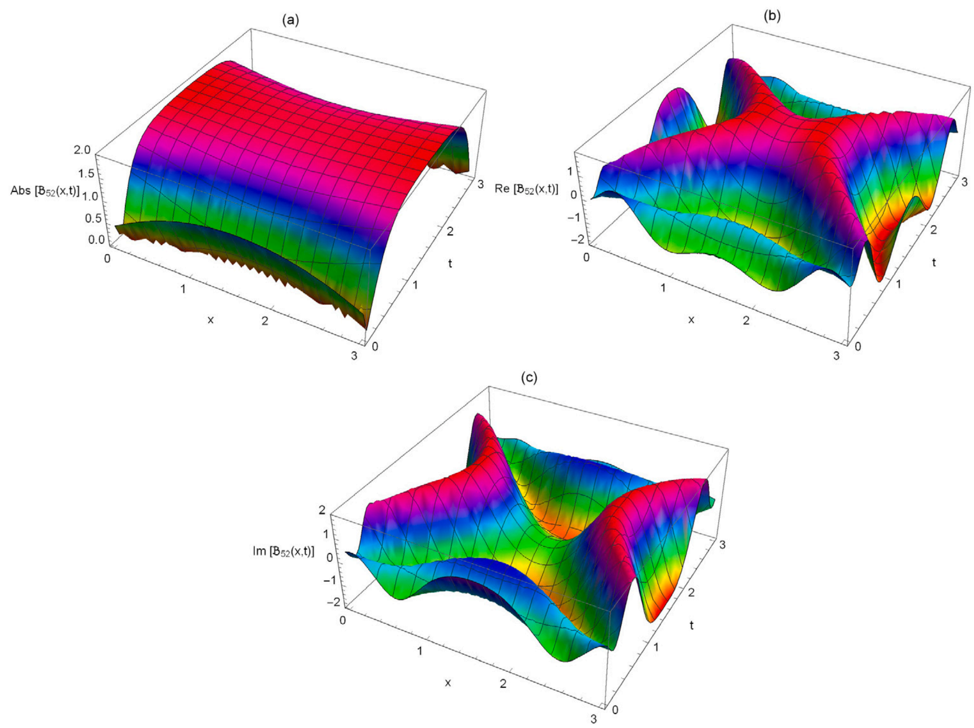

Fig. 15. Numerical simulation of absolute, real, and imaginary Eq. (61) in three-dimensional plots.

$2\Big]$, yields:

$$\mathcal{E} = \frac{1}{r_1}\left[32\left(-\log\left(e^{-5r_1}+5e^5\right)+\log\left(e^{5r_1}+5e^5\right) - \log\left(e^{5r_1+5}+5\right)+\log\left(e^{5-5r_1}+5\right)\right)\right]+800 \tag{71}$$

Thus, we obtain

$$\left.\frac{\partial \mathcal{E}}{\partial r_1}\right|_{r_1=5} = 12.79999964 > 0. \tag{72}$$

This means, this solution is stable.

Investigating the stability of the solution of Eq. (4) by using (57) with the following values of the constants $\Big[a_0 = 1,\ v_2 = 5,\ v_1 = 3,\ v_3 = 2\Big]$, yields:

$$\mathcal{E} = \frac{1}{25r_1}\left[4\left(\log\left(\cosh\left(\frac{5}{2}(r_1-1)\right)\right)-\log\left(\cosh\left(\frac{5}{2}(r_1+1)\right)\right)\right)\right]+2 \tag{73}$$

Thus, we obtain

$$\left.\frac{\partial \mathcal{E}}{\partial r_1}\right|_{r_1=7} = 0.01632653061 > 0. \tag{74}$$

This means, that this solution is stable, and by applying the same steps to other obtained solutions, the stability property of each one of them can be determined.

Remark. We have changed the value of the above-mentioned parameters as following $\Big[a_0 = 9,\ b_0 = 3,\ \eta = 7,\ s_1 = 5,\ s_2 = 6\ \&\ a_1 = 12,\ A = 2,\ b_0 = 7,\ b_1 = 1\ \&\ a_0 = -5,\ v_2 = 6,\ v_1 = 3,\ v_3 = 1\Big]$ the solution is stable, however this does not reflect the stability over all parameter ranges. It is worth to mention that the stability is preserved for wide range of parameter sets.

4. Illustration of the solutions

In this section we plot the obtained solutions are traveling wave solutions.

1. Figs. 1, 2 show the wave solution in three and contour plot respectively for the absolute, real, and imaginary values of (7) for $\Big[a_0 = 4,\ b_0 = \frac{4}{5},\ \eta = 1,\ r_1 = -2,\ r_2 = -3,\ r_3 = 2,\ r_4 = -1,\ s_1 = 5,\ s_2 = 6.\Big]$
2. Figs. 3, 4 show the cone wave solution in three and contour plot respectively for the absolute, real, and imaginary values of (19) for $\Big[a_0 = 4,\ b_0 = \frac{4}{5},\ \eta = 1,\ r_1 = -2,\ r_2 = -3,\ r_3 = 2,\ r_4 = -1,\ s_1 = 5,\ s_2 = 6.\Big]$
3. Figs. 5, 6 show the solitary wave solution in three and contour plot respectively for the absolute, real, and imaginary values of (31) for $\Big[a_0 = 8,\ b_0 = 7,\ \eta = -6,\ r_1 = -5,\ r_2 = -7,\ r_3 = 6,\ r_4 = -4,\ s_1 = 3,\ s_2 = 2.\Big]$
4. Figs. 7, 8 show the periodic solitary wave solution in three and contour plot respectively for the absolute, real, and imaginary values of (36) for $\Big[a_0 = -2,\ b_0 = -3,\ \eta = -5,\ r_1 = 2,\ r_2 = 3,\ r_3 = 5,\ r_4 = 7,\ s_1 = 5,\ s_2 = 6.\Big]$
5. Figs. 9, 10 show the dark solitary wave solution in three and contour plot respectively for the absolute, real, and imaginary values of (44) for $\Big[a_1 = -2,\ A = 1,\ b_0 = 3,\ b_1 = 4,\ r_1 = 2,\ r_2 = 3,\ r_3 = 5,\ r_4 = 7.\Big]$

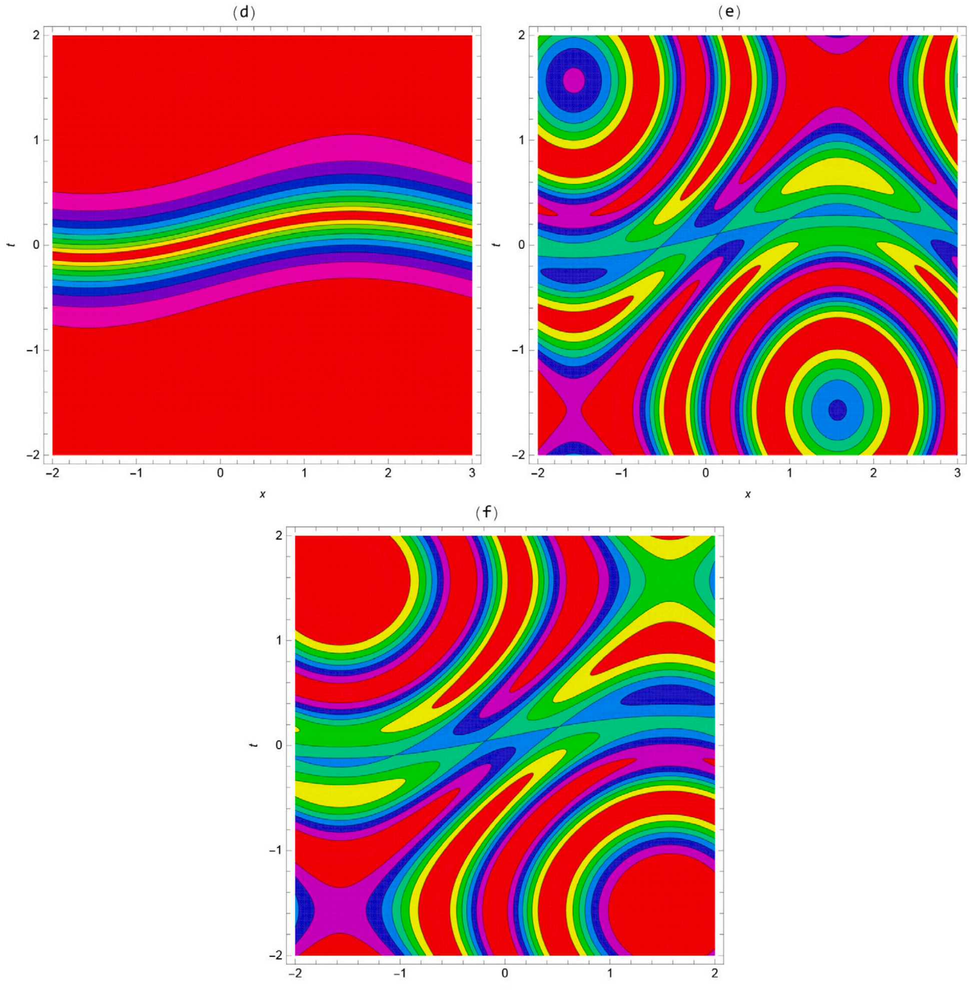

Fig. 16. Numerical simulation of absolute, real, and imaginary Eq. (61) in contour plots.

6. Figs. 11, 12 show the solitary wave solution in three and contour plot respectively for the absolute, real, and imaginary values of (48) for $\left[A = 1,\ q_2 = -4,\ r_1 = 2,\ r_2 = 3,\ r_3 = 5,\ r_4 = 7.\right]$
7. Figs. 13, 14 show the dark solitary wave solution in three and contour plot respectively for the absolute, real, and imaginary values of (57) for $\left[a_0 = 10,\ r_1 = 5,\ r_2 = 6,\ r_3 = 7,\ r_4 = 8,\ \upsilon_2 = 3,\ \upsilon_1 = 2,\ \upsilon_3 = 1.\right]$
8. Figs. 15, 16 show the bright solitary wave solution in three and contour plot respectively for the absolute, real, and imaginary values of (61) for $\left[a_0 = 10,\ r_1 = 5,\ r_2 = 6,\ r_3 = 7,\ r_4 = 8,\ \upsilon_2 = 5,\ \upsilon_1 = 2,\ \upsilon_3 = 3.\right]$

5. The paper novelty

The novelty of our paper, which explains the originality of our results, is discussed in this section. Three recent computational schemes (the extended exp(ϕ)-expansion method, generalized Kudryashov method, and the modified Khater method) are employed to construct distinct types of solutions for the dimensionless form of the Zakharov (ZE) equation. These solutions explain more novel properties for the interaction between (low & high) frequency of (ion-acoustic & Langmuir) waves in plasma. Applying all these schemes to the dimensionless form of the Zakharov equation we deduce that:

1. ***Applied methods:***

   - The modified Khater method reproduces the same results as the extended exp(ϕ)–expansion method For $\left[s_2 = \upsilon_3,\ s_3 = \upsilon_1,\ s_1 = \upsilon_2,\ \Gamma = e,\ e^{\phi(\mathfrak{F})} = \Gamma^{\mathfrak{F}(\mathfrak{F})}\right]$.
   - The modified Khater method reproduces the same results as the generalized Kudryashov method when $\left[\Gamma^{\mathfrak{F}(\mathfrak{F})} = \mathfrak{Q}(\mathfrak{F}),\ \upsilon_1 = 0,\ \upsilon_3 = 1,\ \upsilon_2 = -1\right]$.

2. ***Obtained solutions***

   - According to the equivalence between these methods some of the obtained solutions are leading to recover the solutions obtained in all previous research papers with this model.
   - Comparison between our obtained solutions and that have been collected in [42,43,46–48], shows that our paper where our obtained solutions are recovering these obtained solutions in these papers. Moreover, we note that we have determined novel solutions of this model have been never found previously.

6. Conclusion

In the dimensionless shape of the Zakharov (ZE) equation, multi-soliton waves, periodic waves, dark waves, light waves, and wave solutions have been derived. To analyze new dynamic and physical actions of the interaction between (low & high) frequency and (ion-acoustic & Langmuir) waves in plasma, three recent analytical schemes have been used. The stability property of the obtained solutions has been tested. Several figures have been plotted to illustrate the dynamics of the solutions in the three-dimensional and contour map. We have recovered the previous solutions of this model and we have derived new exact solutions in closed-form that never been generated previously.

CRediT authorship contribution statement

Mostafa M.A. Khater: Conceptualization, Data curation, Formal analysis, Funding acquisition, Investigation, Methodology, Project administration, Resources, Software, Supervision, Visualization, Writing - original draft, Writing - review & editing. **Raghda A.M. Attia:** Conceptualization, Data curation, Formal analysis, Funding acquisition, Methodology, Project administration, Visualization, Writing - original draft, Writing - review & editing. **Emad E. Mahmoud:** Data curation, Investigation, Resources, Software, Supervision, Writing - review & editing. **Abdel-Haleem Abdel-Aty:** Conceptualization, Data curation, Funding acquisition, Methodology, Project administration, Software, Validation, Visualization, Writing - review & editing. **Kholod M. Abualnaja:** Formal analysis, Funding acquisition, Investigation, Resources, Supervision, Visualization, Writing - review & editing. **A.-B.A. Mohamed:** Formal analysis, Investigation, Validation, Writing - review & editing. **Hichem Eleuch:** Formal analysis, Methodology, Software, Validation, Writing - review & editing.

Declaration of competing interest

The authors declare that they have no known competing financial interests or personal relationships that could have appeared to influence the work reported in this paper.

Acknowledgments

Taif University Researchers Supporting Project number (TURSP-2020/20), Taif University, Taif, Saudi Arabia.

References

[1] Hosseini K, Mayeli P, Ansari R. Modified Kudryashov method for solving the conformable time-fractional Klein–Gordon equations with quadratic and cubic nonlinearities. Optik 2017;130:737–42.
[2] Ellahi R, Fetecau C, Sheikholeslami M. Recent advances in the application of differential equations in mechanical engineering problems. Math Probl Eng 2018;2018:1584920.
[3] Guy TT, Bogning JR. Modeling nonlinear partial differential equations and construction of solitary wave solutions in an inductive electrical line. J Adv Math Comput Sci 2019;33:1–10.
[4] Zhang X, Sagiya T. Shear strain concentration mechanism in the lower crust below an intraplate strike-slip fault based on rheological laws of rocks. Earth Planets Space 2017;69(1):82.
[5] Hosseini K, Mayeli P, Ansari R. Modified Kudryashov method for solving the conformable time-fractional Klein–Gordon equations with quadratic and cubic nonlinearities. Optik 2017;130:737–42.
[6] Kumar D, Singh J, Prakash A, Swroop R. Numerical simulation for system of timefractional linear and nonlinear differential equations. Prog. Fract. Differ. Appl. 2019;5:65–77.
[7] Hasanov A, Choi J. Note on Euler–Bernoulli equation. Sohag J Math 2020;7(2):33–6.
[8] Delkhosh M, Parand K. A hybrid numerical method to solve nonlinear parabolic partial differential equations of time-arbitrary order. Comput Appl Math 2019;38(2):76.
[9] Khater M, Attia R, Abdel-Aty A. Computational analysis of a nonlinear fractional emerging telecommunication model with higher–order dispersive cubic–quintic. Inf Sci Lett 2020;9:83–93.
[10] Khater MM, Seadawy AR, Lu D. Dispersive optical soliton solutions for higher order nonlinear Sasa-Satsuma equation in mono mode fibers via new auxiliary equation method. Superlattices Microstruct 2018;113:346–58.
[11] Alabau-Boussouira F, Ancona F, Porretta A, Sinestrari C. Trends in control theory and partial differential equations, vol. 32. Springer; 2019.
[12] Lin H. Electronic structure from equivalent differential equations of Hartree–Fock equations. Chin Phys B 2019;28(8):087101.
[13] Pels A, Gyselinck J, Sabariego RV, Schöps S. Solving nonlinear circuits with pulsed excitation by multirate partial differential equations. IEEE Trans Magn 2017;54(3):1–4.
[14] Nchama GAM, Mecıas AL, Richard MR. The caputo-fabrizio fractional integral to generate some new inequalities. Inf Sci Lett 2019;8:73–80.
[15] Cevikel AC. New exact solutions of the space–time fractional KdV-Burgers and nonlinear fractional foam Drainage equation. Therm Sci 2018;22(Suppl. 1):15–24.
[16] Raissi M. Deep hidden physics models: Deep learning of nonlinear partial differential equations. J Mach Learn Res 2018;19(1):932–55.
[17] Abdel-Aty A, Zakaria N, Cheong LY, Metwally N. Quantum network via partial entangled state. J Commun 2014;9:379–84.
[18] Abdel-Aty M, Abdalla MS, Obada A-SF. Entropy and phase properties of isotropic coupled oscillators interacting with a single atom: one-and two-photon processes. J Opt B: Quantum Semiclass Opt 2002;4:S133–41.
[19] Abdel-Aty A, Zakaria N, Cheong LY, Metwally N. Effect of the spin–orbit interaction on partial entangled quantum network. Lect Notes Electr Eng 2014;285:529.
[20] El-Shahat TM, Abdel-khalek S, Abdel-aty M, Obada ASF. Entropy squeezing of a degenerate two-photon process with a nonlinear medium. J Modern Opt 2003;50:2013–30.
[21] Feerman CL, Robinson JC, Rodrigo JL, Diez JLR. Partial differential equations in fluid mechanics, vol. 452. Cambridge University Press; 2018.
[22] Ismail G, Abul-Ez M, Farea N. An accurate analytical solution to strongly nonlinear differential equations. Appl Math Inf Sci 2020;14:141–9.
[23] Sun G-Q. Mathematical modeling of population dynamics with Allee effect. Nonlinear Dynam 2016;85(1):1–12.
[24] Lopatiev A, Ivashchenko O, Khudolii O, Pjanylo Y, Chernenko S, Yermakova T. Systemic approach and mathematical modeling in physical education and sports. J Phys Educ Sport 2017;17(1):146–55.
[25] Zhang P, Xiao X, Ma Z. A review of the composite phase change materials: Fabrication, characterization, mathematical modeling and application to performance enhancement. Appl Energy 2016;165:472–510.
[26] Park C, Khater MM, Abdel-Aty A-H, Attia RA, Rezazadeh H, Zidan A, et al. Dynamical analysis of the nonlinear complex fractional emerging telecommunication model with higher–order dispersive cubic–quintic. Alexandria Eng J 2020;59(3):1425–33.
[27] Attia RA, Lu D, Ak T, Khater MM. Optical wave solutions of the higher-order nonlinear Schrödinger equation with the non-kerr nonlinear term via modified Khater method. Modern Phys Lett B 2020;34(05):2050044.
[28] Ali AT, Khater MM, Attia RA, Abdel-Aty A-H, Lu D. Abundant numerical and analytical solutions of the generalized formula of Hirota–Satsuma coupled KdV system. Chaos Solitons Fractals 2020;131:109473.
[29] Khater MM, Attia RA, Abdel-Aty A-H, Abdou M, Eleuch H, Lu D. Analytical and semi-analytical ample solutions of the higher-order nonlinear Schrödinger equation with the non-Kerr nonlinear term. Results Phys 2020;16:103000.
[30] Khater MM, Park C, Abdel-Aty A-H, Attia RA, Lu D. On new computational and numerical solutions of the modified Zakharov–Kuznetsov equation arising in electrical engineering. Alexandria Eng J 2020;59:1099–105.
[31] Park C, Khater MM, Attia RA, Alharbi W, Alodhaibi SS. An explicit plethora of solution for the fractional nonlinear model of the low–pass electrical transmission lines via Atangana–Baleanu derivative operator. Alexandria Eng J 2020;59:1205–14.
[32] Khater MM, Alzaidi J, Attia RA, Lu D, et al. Analytical and numerical solutions for the current and voltage model on an electrical transmission line with time and distance. Phys Scr 2020;95(5):055206.
[33] Khater MM, Attia RA, Baleanu D. Abundant new solutions of the transmission of nerve impulses of an excitable system. Eur Phys J Plus 2020;135(2):1–12.
[34] Li J, Attia RA, Khater MM, Lu D. The new structure of analytical and semi-analytical solutions of the longitudinal plasma wave equation in a magneto-electro-elastic circular rod. Modern Phys Lett B 2020;2050123.
[35] Yue C, Khater MM, Attia RA, Lu D. The plethora of explicit solutions of the fractional KS equation through liquid–gas bubbles mix under the thermodynamic conditions via Atangana–Baleanu derivative operator. Adv Difference Equ 2020;2020(1):1–12.
[36] Khater MM, Park C, Lu D, Attia RA. Analytical, semi-analytical, and numerical solutions for the Cahn–Allen equation. Adv Difference Equ 2020;2020(1):1–12.
[37] Ghanbari B, Kumar S, Kumar R. A study of behaviour for immune and tumor cells in immunogenetic tumour model with non-singular fractional derivative. Chaos Solitons Fractals 2020;133:109619.
[38] Liu Q, Zhang R, Yang L, Song J. A new model equation for nonlinear Rossby waves and some of its solutions. Phys Lett A 2019;383(6):514–25.
[39] Liu Q, Chen L. Time-space fractional model for complex cylindrical ion-acoustic waves in ultrarelativistic plasmas. Complexity 2020;2020:9075823.

[40] Eleuch H, Rostovtsev YV, Scully MO. New analytic solution of Schrödinger equation. Europhys Lett 2010;89(5):50004.
[41] Jha PK, Eleuch H, Rostovtsev YV. Analytical solution to position dependent mass Schrödinger equation. J Modern Opt 2011;58:652–6.
[42] Biswas A, Zerrad E. 1-soliton solution of the Zakharov–Kuznetsov equation with dual-power law nonlinearity. Commun Nonlinear Sci Numer Simul 2009;14(9–10):3574–7.
[43] Janssen PA, Onorato M. The intermediate water depth limit of the Zakharov equation and consequences for wave prediction. J Phys Oceanogr 2007;37(10):2389–400.
[44] Yang X-l, Tang J-s. Explicit exact solutions for the generalized Zakharov equations with nonlinear terms of any order. Comput Math Appl 2009;57(10):1622–9.
[45] Wazwaz A-M. The extended tanh method for abundant solitary wave solutions of nonlinear wave equations. Appl Math Comput 2007;187(2):1131–42.
[46] Akbar MA, Ali NHM, Hussain J. Optical soliton solutions to the (2 + 1)-dimensional Chaffee infante equation and the dimensionless form of the Zakharov equation. Adv Difference Equ 2019;2019(1):446.
[47] Ebadi G, Krishnan E, Biswas A. Solitons and cnoidal waves of the Klein–Gordon–Zakharov equation in plasmas. Pramana 2012;79(2):185–98.
[48] Sun J, Yao S, Wu T-f. The stationary quantum Zakharov system perturbed by a local nonlinearity. Appl Math Lett 2019;95:172–8.